Soft Psychophysiology:
An Investigation of Soft Robotic Sensors as Psychophysiological Measuring Tools

May 17th, 2020

Team Members

Ryan Breuer
Shannon Carey
Samuel Milender

WPI Advisors

Jeanine Skorinko
Cagdas Onal

Abstract

Psychophysiology uses physiological data to gain insights into psychological states, such as sweat indicating anxiety or facial tics when repressing bias. One such measure, electromyography (EMG), detects muscular movements through reading electrical impulses beneath the skin. Unfortunately, many EMG devices experience problems such as high signal noise, prohibitive setups, and high costs that restrict study design. Our project applied new technologies from soft robotics to develop an alternative to EMG. While a full study was not possible, testing of our device suggested that flexible embedded fluid sensors could function in place of EMG when examining participant stress through the trapezius muscle, and our cost analysis suggests they are significantly less expensive.

Table of Contents

Introduction

As we move into a period in history more and more driven by data, the field of psychophysiology has become an increasingly popular supplement to traditional psychological testing methods. Psychophysiology is the attempt to measure mental states through different physical responses. This means capitalizing on indicators like sweaty palms or facial tics.

While these advances are significant, the field still has a long way to go, and many of the devices that currently exist to extract physiological data experience a number of problems, such as high signal noise and prohibitive setups that don't allow study participants to move around freely. While a few companies have managed to move past these barriers, their products are typically prohibitively expensive. This significantly limits who can use these devices and how they get used in psychophysiological research.

Our project seeks to narrow in on one particular instance of a biosensor being used for psychophysiological measurement, and to explore alternatives from the rising field of soft robotics. This new "soft" technology consists of actuators and sensors that can bend as needed while still retaining functionality. This quality of deformation lends soft robotic sensors to be used in situations where fragile objects or objects of an unknown shape or size are involved. These sensors are capable of understanding multi-axis strain and high-precision, low force pressure, using a combination of conductive liquids and rubbers/silicone (Sensors, n.d.).

While soft robotic sensors do not detect muscular movement in the same way that electromyographic data does, we hypothesize that these sensors could detect muscle movement to a similar precision, but without the errors caused by the inherent noise of electromyography. Much of the data gathered by electromyography is more detailed than necessary for many

psychophysiological applications, so by measuring the muscle's physical contraction rather than the nerve impulses sent to the muscle to cause contraction, extraneous and confusing data are avoided. This project seeks to employ soft robotics sensors as an alternative to Trapezius electromyography in psychophysiological studies of stress. We aim to discern their viability and realistic precision in this application.

To this end, this report details the development of a soft robotic sensor device capable of measuring macro muscle movements. The overall goal is to work towards a device which costs less, is easier for participants and researchers to use, and produces cleaner data. This is done in an effort to increase the accessibility of psychophysiology research, to promote and facilitate its use in studies which could contribute positively to mental and physical health research.

Background

To effectively understand the purpose behind this project, we must make sure that certain background information is known. The core purpose of this project lies in the field of psychophysiology. The intent is to design and fabricate a device that can be compared to traditional psychophysiological measures like Electromyography (EMG). This type of sensor can be used to measure how a multitude of different psychological stimuli induce a multitude of different responses from different muscle groups. For many of these, the use of mechanical sensors is impractical, so we must determine what type of stimuli can be used to induce a muscular response to be measured by the device. We must then determine what kind of sensor would best measure the kinds of responses we decide to induce. The following is an outline of the background information used to inform these decisions.

Psychophysiological Measures and Project Scope

To gain a more comprehensive grasp of the problems inherent in today's available psychophysiology tools, we explored available resources and reviewed a body of scientific literature. Our exploration involved a parallel search through a number of different psychophysiological measures (tools and techniques for collecting biological indicators) and psychological constructs (emotional states).

The three most commonly referenced measuring tools were EMG, Galvanic Skin Response (GSR), and Heart Rate. Of these, EMG held the best combination of traits to be the subject of our study; while EMG is used in a myriad of contexts, from medical devices and muscular rehabilitation to research on stress and implicit bias, it suffers from a wealth of well-documented problems, with effective devices costing up to $20,000 for a kit (Pizzolato et

al., 2017). To get a better sense of how EMG is used in psychology, we further explored the science behind this technology and documented its most common applications in research.

What is Electromyography?

Electromyography is the study of muscle movement through the analysis of a muscle's electrical signals. When a motor neuron is stimulated, it releases calcium ions, which depolarize and thereby tense the muscle (Farnsworth, 2019). This depolarization creates an electromagnetic field, which registers on electromyographic tools as a voltage (Rash, n.d.). In the context of psychology, muscle movements can be indicative of emotional reactions. On a very explicit level, this can be something as straightforward as someone's cheek muscles moving when they smile, but micro-movements and tensions have also been demonstrated to correlate with certain emotions as well, such as stress being reflected in shoulder tension (Larson, et. al., 1995). In this way, electromyography can be used on a number of different muscle groups to detect a multitude of emotional contexts and valances, such as disgust, joy, or anger (Vrana, 1993). Electromyography can even be used to detect minute muscle movements where no visual change occurs, such as in facial EMG (Farnsworth, 2019). Being able to quantify and record minute reactions allows researchers to understand a person's physiological state as it changes in response to stimuli. These states can be powerful tools to study what's actually going on in a participant's head, even when that participant may be themselves unaware of it. This helps researchers to examine topics such as implicit bias and suppressed emotions in ways not previously possible, as well as verify participant self-reports to account for the inherent difficulty of self-assessment.

Challenges of Using EMG

EMG is a useful tool for psychologists, but as a technology, it still has a long way to go. Almost every article or guide discussing this tool prominently features a section on the dangers and difficulties of parsing through potentially erroneous data. One source identifies as many as seven categories of data artifacts that might occur when using EMG, with each one having specific (and challenging) filtering strategies or preparation techniques to combat it (Chowdhury, 2013). While psychophysiology provides useful objective measures when used successfully, the difficulties presented in their appropriate use makes them less reliable. The data experimenters can get from it is valuable, but that's only if they can get that data successfully. This undermines what could have been a remarkable source of information, and for this reason amongst others, numerous EMG studies result in inconclusive evidence (Subbu, 2015).

Trapezius EMG and Stress

Stress is a topic of significant interest for psychologists, given its massive prevalence in people of all demographics. Stress can be defined as a situation where not enough resources are available for a person to meet the given environmental and social demands (Frankenhaeuser 1989 as cited in Lundberg, 1999). Psychosocial factors have been demonstrated to influence a number of somatic and mental health problems through their chemical and hormonal manifestations. Stress has been observed to contribute to impaired immune-response, depression, musculoskeletal disorders, and cardiovascular disease (Lundberg 1999).

The ability to quantify stress effectively is critical to developing interventions to many of these health effects. Psychophysiological tools, at their most basic level, measure some sort of emotional arousal, and often reflect physical manifestations of the "fight or flight" response of the body, making them ideal for basic stress responses. One study discussing the use of EMG and ECG (electro-cardiogram) found that distinctly different patterns arose in signal amplitudes during stress conditions (i.e., calculation tasks, logic puzzles, memory tasks) as opposed to rest (Wijsman et. al., 2013). Similar findings were produced as participants reacted to a Stroop Color-Word Test when using trapezius EMG and Laser-Doppler Flowmetry (Larsson, et. al., 1995), as well as heart rate, blood pressure, urinary catecholamines, salivary cortisol, and trapezius EMG (Lundberg, 1994).

Our Decision to Study EMG in Stress Research

Beyond stress, there are a variety of different psychological topics currently researched (in part) using EMG as a methodological tool. Anxiety studies have made use of EMG sensors measuring the response of the frontalis muscle beneath the forehead (Hoehn-Saric, 1989). Depression studies have likewise measured the zygomaticus major and corrugator supercilii, two other facial muscle pairs (Benning & Oumeziane, 2017). One value of using EMG is its ability to pick up micro-muscular movements which often reflect almost no visible macro-scale changes. This resolution is crucial for measuring the activity of small muscles. At the moment, soft sensors have no capacity to replicate this technology.

Trapezius tension and motion, however, are easily detected on a larger scale. EMG use in a study requiring these measurements could feasibly be replaced by a much less expensive soft sensor, and with better noise yield. While EMG can measure the trapezius without issue, the sensitivity required for micro-movements is unnecessarily precise when applied to something as

large-scale as a shoulder, and leads to more error than needed. Because of this, we believe it reasonable that a soft sensor would function as an acceptable alternative in this situation.

A summary of selected psychophysiology study types, along with some of their common measurement locations, is listed in Table 1. The third column lists our subjective judgements regarding the difficulty posed in replicating such a study, if soft sensors were substituted for EMG. These judgements are primarily based on the size of the associated muscle groups, the feasibility of non-invasively attaching a sensor to the respective location, and the complexity of the associated study methodology.

Study	Measurement Location	Study Difficulty
EMG Stress	Trapezius	Easy
EMG Anxiety	Frontalis, Corrugator supercilii	Hard
EMG Depression	Paraspinal, Frontalis	Hard
EMG Valence	Zygomaticus major, Corrugator supercilii	Moderate

Table 1. Psychophysiological Measures

Trapezius Anatomy and Physiology

Due to the physiological nature of this project, a baseline understanding of relevant anatomical structures and their function is required. In order to measure the contraction of the trapezius, we need to determine two fixed points on the skeleton between which to measure. The contraction of the trapezius should change the distance between the fixed points, and in measuring that change in distance we can measure the muscle's contraction. The most effective places for these fixed points are on or near the "point of origin" of the muscle (the part of the skeleton that stays stationary when the muscle contracts) and one on or near its "point of

insertion" (the part of the skeleton that moves when the muscle contracts). The distance between these two points will see the most drastic change as the muscle contracts.

Superior Trapezius

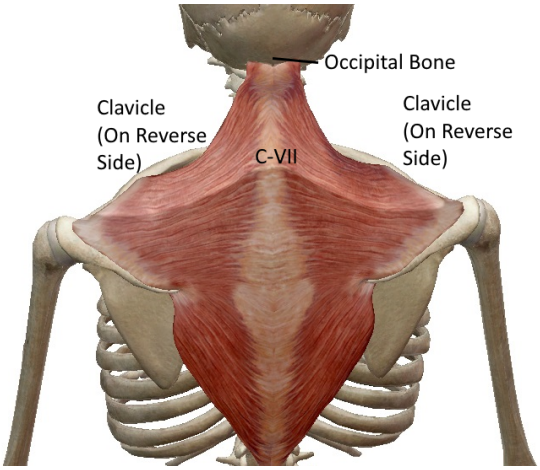

Figure 1: The superior Trapezius fibres with their "points of origin" and "points of insertion" labeled. Argosy Publishing, *Trapezius*. Retrieved from https://cervicalspine.wordpress.com/anatomy/myology/.

The "points of origin" of the superior trapezius fibres are between the occipital bone of the skull and the vertebra C-VIII, and their "points of insertion" are along the outer third of the clavicle (Figure 1). The longest fibres are between C-VIII and the outermost point of the clavicle, called the "acromion process". (Gorman, 2020).

Medial Trapezius

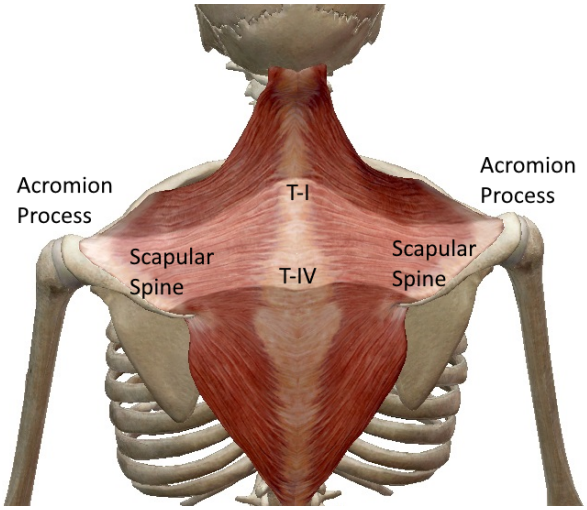

Figure 2: The medial Trapezius fibres with their "points of origin" and "points of insertion" labeled. Argosy Publishing, *Trapezius*. Retrieved from https://cervicalspine.wordpress.com/anatomy/myology/.

The "points of origin" of the medial trapezius fibres are between the vertebrae TI and TIV, and their "points of insertion" are at the acromion process and extend along the scapular spine (Figure 2). The longest fibres are between vertebra T-I and the Acromion Process (Gorman, 2020).

Soft Robotics Sensors

Our first step in approaching an alternative device for measuring stress through trapezius movement was to assess what sensors are available to us. Two of the three main families of sensors were immediately eliminated from our options, as their primary functions were entirely different from our needs. Planar deformation and bladder deformation sensors both deal with touch and pressure, neither of which can measure muscle contraction. This left the third group, lateral deformation sensors, which suited our design needs because they specialize in stretching along an axis.

In order to determine which of these lateral deformation sensors may be used to measure the aforementioned muscle contractions, it is important to first determine what types of sensors exist. For this purpose, four different types of sensors are explored: flexible embedded liquid strain sensors, Smart Braid sensors, dielectric elastomer sensors, and refraction deformation sensors. In considering the pros and cons of each type of sensor, the most effective one for the purposes of this project can be determined.

Flexible embedded liquid strain sensors (eGaIn, KI-Gly, etc.)

As a piece of elastomeric substance is stretched, it both elongates in the direction of stretch and shrinks in the two perpendicular dimensions. Any channels within the elastomer, in the direction of stretch, proportionately elongate and narrow. If the channels contain a conductive fluid, the electrical resistance through the fluid increases as the channels holding it extend according to the following formula: $\Delta R = \frac{\rho \varepsilon L(8-\varepsilon)}{wh(2-\varepsilon)^2}$, where ΔR is the change in resistance, ρ is the resistivity of the fluid, ε is the strain applied to the sensor, L is the overall length of the internal channels, w is the width of the internal channels, and h is the height of the internal channels. This change in resistance can be related to how far the elastomer has been stretched. Sensors relying on this technology typically consist of two cast silicone halves that, when put together, form a series of looping channels. To convert those channels into “wires”, they are filled with a conductive fluid, e.g. eutectic Gallium Indium (eGaIn), Potassium Iodide Glycerol (KI-Gly), or simple aqueous solution of distilled water and non-iodized sodium chloride, or table salt (aqNaCl). Lastly, diodes or circuits are fitted to the sensor, both acting as caps on either end of the channels and as a means through which the change of resistance can be measured (Figure 3).

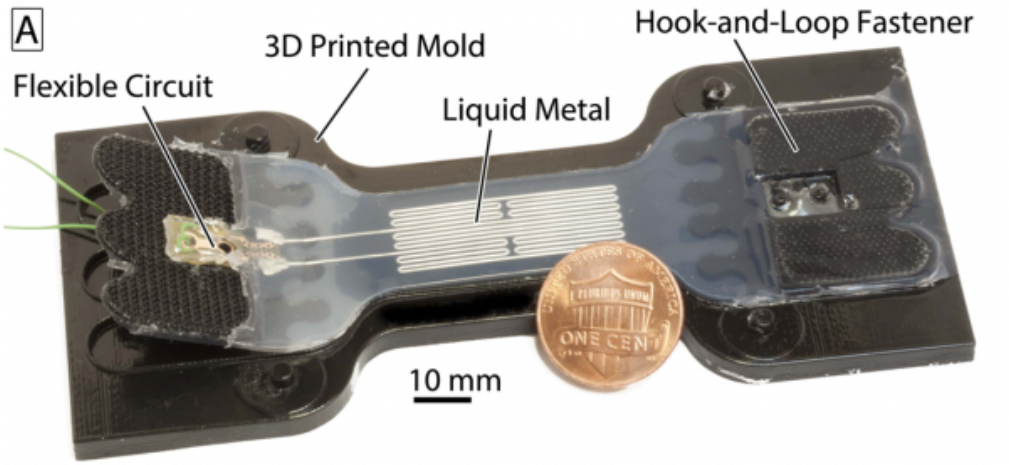

Figure 3: A Typical eGaIn Sensor, though the Design of KI-Gly or aqNaCl is Identical. Soft Robotics Toolkit, *eGaIn Sensors*. Retrieved from https://softroboticstoolkit.com/book/egain-sensors.

The fabrication of these types of sensors allows them to be customized easily, as they are silicone castings. Their shape and dimensions are entirely dictated by molds that are easily fabricated by stereolithography, a rapid-prototyping method available to us. Therefore, a sensor ideal for the purposes of the required application can be developed through iterative testing.

The main downside to using flexible embedded strain sensors in this application is the process of securing them to a person. From the relaxed state, they are only able to measure elongation, not contraction. In order to get an accurate reading of the motion of the trapezius, the sensor needs to be fixed to a study participant such that, when they tense their shoulders, the sensor remains under tensile stress as it is allowed to shorten. If the sensor is completely relaxed (i.e. loose) at the point of least tension, the sensor will not be able to read accurately. Affixing the sensor while it is under strain to the subject while their shoulders are at a neutral position will be simple, but creating a method by which the two ends of the sensors do not move from their proper positions on the participant's back while the sensors are constantly under strain will be challenging (Soft Robotics Toolkit, eGaIn sensors, n.d.).

Smart Braid Sensors

Smart braids use changes in inductance across woven wires to measure the deformation of structures. Generally these wires are woven into a cylinder surrounding a pneumatic muscle to measure deformation. This same technique, if woven around any elastomer core, could measure how far the elastomer is being stretched.

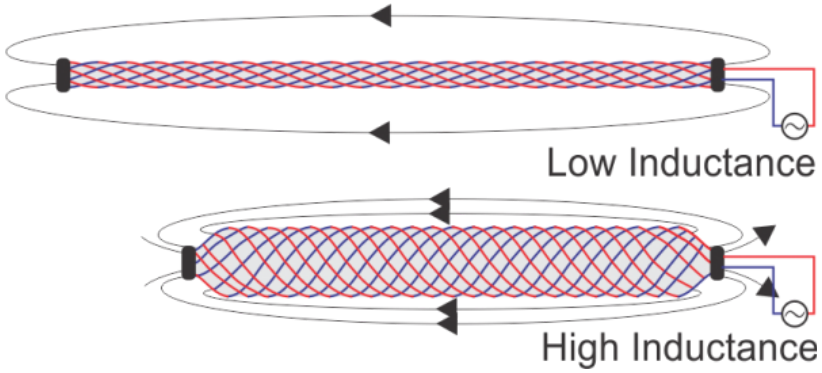

Figure 4: The typical design of a Smart Braid. Soft Robotics Toolkit, *Smart Braids*. Retrieved from https://softroboticstoolkit.com/smart-braids.

As the elastomer core is subjected to strain, it will narrow in proportion to how much it stretches. The changes in dimension of the core will change the geometry of the wire braid, which will change the angle each wire makes with overlapping wires. This change in angle causes a change in inductance, which can be measured and related back to the amount of strain being applied to the elastomer core (Figure 4).

This system can be used to measure the change in length of any constant-diameter elastomer core, meaning customization for the desired application is simple. The elastomer can be formed in any shape allowing for it to follow the natural curves of human muscles, and by fixturing each end of the sensor (by means of some garment or harness) to the correct places on the participant's back, could easily mimic the strain as it is applied to the superior trapezius.

The biggest challenge in using Smart Braids is that compared to resistance, inductance is harder to measure directly. Inductance is represented by the formula $V = L\frac{dI}{dt}$, where V is voltage, L is inductance, and $\frac{dI}{dt}$ is the change in current. As most electrical systems can only read voltage, this would require specific circuit elements to be set up to calculate for the actual inductance. In a real-time system, this would also mean doing a significant amount of math every time you wanted to produce a reading. It is also feasible to use a signal generator with a known signal to obtain essentially the transform function of the system, but this would require a signal generator and an in-depth model of how the elastomer stretches. While none of these are impossible to obtain, the signal generator may require the system to exceed its size, weight, and/or power constraints because measuring current over time at the speed required might be challenging (Soft Robotics Toolkit, Smart Braids, n.d.).

Dielectric Elastomers

Dielectric elastomers operate around yet another key electrical principle, as a type of elastic variable capacitor. They consist of a sheet of an elastomer with a coating of an electrically conductive substance on either side of it (Figure 5).

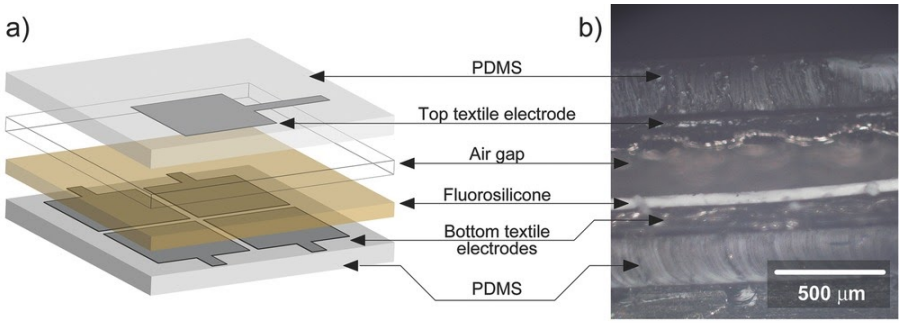

Figure 5: The typical design of a dielectric elastomer sensor (Carey, 2020).

As the elastomer is put under strain, it becomes narrower, bringing the two electrically conductive surfaces closer together. This causes their capacitance to increase, which can be associated with the strain applied to the elastomer to measure the change in length. This can be

modeled by the formula $C = \frac{\varepsilon A}{d}$, where A is the plate area, d is the distance between plates, and epsilon is the membrane permittivity.

Dielectric elastomers are very pliable. They are flat, so they would not break the desired form factor of the sensor, and could be moulded to the shape of the trapezius. They also can be manufactured at different sensitivity ranges, which is useful for engineering a specific sample for a specific application.

The biggest problem with dielectric elastomers is the challenges they face in reflecting a sustained measurement. Because capacitance is a measure of the change in voltage, not absolute voltage, a capacitance-based sensor will only be able to pick up moments of fluctuation in data. In our application, this means that if the participant was continually tensing and relaxing their shoulders, we would see lots of change, but if tension increased and then stabilized at that new value, the reading would "disappear". Secondarily, though with no less importance, is the fact that many currently existing dielectric elastomers use massive voltages to achieve any sort of readable measurement. This makes them dangerous to use around human beings, even if precautions are taken (Carey, 2019).

Refraction Deformation Sensors

Refraction deformation sensors are an interesting subset of soft sensors, insofar as they do not take advantage of a basic electric property. Instead, they use the refraction of light. To fabricate one of these sensors, an optical cable has a pattern marked on it called Fiber Bragg Grating. When a beam of light is shone through the pattern in the cable and it is under bending stress, it will reflect some wavelengths of light and transmit the rest. Comparing the input frequency and output frequency of light in these sensors can be used to determine by how much the cable is being deformed, and in some cases, where and in what direction. Unfortunately

these sensors, while very good at what they do, must be excluded from consideration as they only measure bending strain, rather than the lateral strain that is caused by the contraction of muscles (Carey, 2019).

Methodology

This project consists of four main parts: the sensors to read the Trapezius connections, the electronics to capture and store those readings, the harness to fixture the sensors to the body, and the tests to ensure that each part of the project works as intended. The sensors, electronics, and harness assemble into the device whose objective is to provide sensor data for psychophysiological readings. It should remain safe under normal operating conditions, as well as a predicted safety factor, be effective on a variety of body types and sizes, should be intuitive to use for the average participant and researcher, and affordable to purchase or fabricate.

The Sensors

The most crucial part of the project rests with the sensors. They provide the psychophysiological data that will support or refute our hypothesis. The following outlines the process of analyzing several different types of sensors to choose a single type to use, the design of the type of sensor chosen, and its fabrication.

Sensor Selection

To make our final selection of a sensor for this application, a matrix of sensor traits was compiled. The matrix takes into account the following characteristics: the sensor type's measurement type, range, and resolution; its electrical requirements; its availability or manufacturability; and its safety.

Measurement type + Range/Resolution. How effective the sensor is in detecting muscle contraction (type of measurement, resolution, etc.) is evaluated in the "Measurement" column of the matrix.

Electrical Requirements. How much power, current, or voltage is required for the sensor to take a reading and how much additional circuitry is required for the sensor's function are attributes evaluated in the "Electrical Requirements" column of the matrix.

Availability/Manufacturability. How easily the sensor may be obtained or fabricated is evaluated in the "Availability/Manufacturability" column of the matrix.

Safety. How much risk the sensor poses to the health or safety of the human participants when used in direct or close contact with the body is evaluated in the "Safety" column of the matrix.

These characteristics were evaluated for each sensor type and are used in a decision matrix to determine the most effective sensor to use for the purposes of this study (Table 2).

Sensor Type	Measurement	Electrical Requirements	Availability / Manufacturability	Safety
Flexible Embedded Fluid	Linear Strain	Minor	Reasonable	Safe
Pneumatic Deformation	Pressure	Minor	Prohibitive	Safe
Smart Braid	Linear Strain	Moderate	Moderate	Safe
Dielectric Elastomers	Planar or Linear Strain	Significant	Prohibitive	Unknown
Refraction Deformation	Linear Deflection	Minor	Prohibitive	Safe

Table 2: The Sensor Decision Matrix.

Design Constraints, Functional Specifications, and Materials

The family of flexible embedded fluid sensors were selected, but the creation and fabrication of a specific design was required for this application. The sensors must provide precise and repeatable electrical data in response to the strains present as the human body moves through its range of motion. The sensors must be capable of mounting and being removed from the body of the participant such that its position is consistent. The sensors must operate entirely within their elastic range, with a safety factor such that fatigue is mitigated and creep is avoided. The sensors must not bind up or be caught significantly on fabric clothing, in order to ensure even stretching and deformation.

This family of sensors is usually fabricated by casting and laminating elastomer layers. Since a wide variety of shapes and thicknesses are available with this method, the sensor design is primarily constrained by the properties of the available materials. In background research, it was clear that the primary mode of failure for successful sensors was delamination at the sensor/base interface, due to the large jump in stiffnesses (Sensors, n.d.). This problem is usually addressed by the use of an elastomer of intermediary stiffness between the sensor ends and main flexible body (Figure 6).

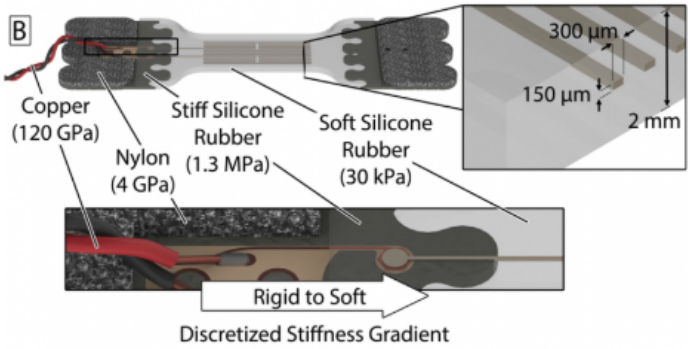

Figure 6: Stiffness gradients in flexible embedded fluid sensors Soft Robotics Toolkit | eGaIn Fabrication, *Diagram of Full Sensor*. Retrieved from https://softroboticstoolkit.com/book/egain-fabrication.

In the final design of our sensors, the problem was addressed instead by the geometry of the mechanical configuration. The sensor was designed such that the width of the anchor ends

was four times that of the width of the main body section, in order to distribute the majority of the strain and associated forces away from the sensor junctions. This allowed for the selection of a single elastomer, Ecoflex 00-30 (1.3 kpa elastic modulus), as the sensor body material (Smooth-On, n.d.). Nylon strapping was selected for the sensor ends due to its successful use in previous sensor research, and compatibility with the overall device design. A completed sensor of this design is shown in Figure 7.

Stainless steel hook and eye closures were selected as the sensor fixturing method, with a pair used at each anchoring location. They allow for a very rigid fixture that can also be easily taken on and off , while also being extremely inexpensive.

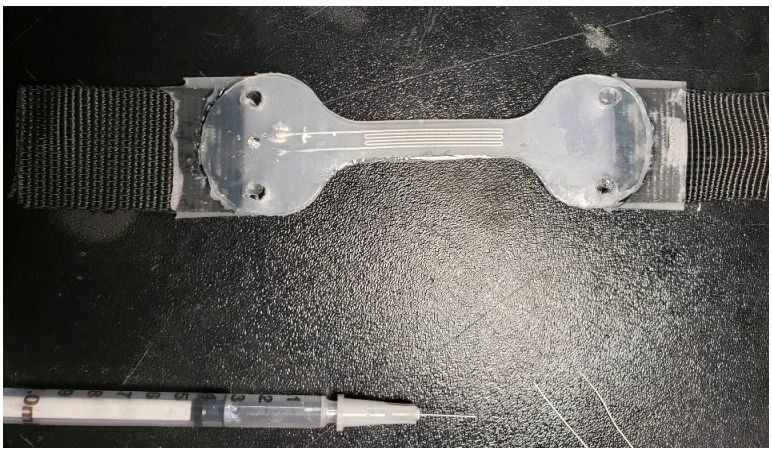

Figure 7: Final manufactured sensor, with no stiffness gradient.

Two different conductive fluids were selected for eventual comparative testing within the sensors. The first was eGaIn, a eutectic, liquid alloy of gallium and indium, with resistivity $\rho = (29.4 \times 10{-}8\ \Omega{\cdot}m)$. The second was KI-Gly, an electrolytic solution of X% potassium iodine in glycerol. Both fluids were compatible with the initial mechanical configuration.

Sensor Fabrication

The required flexible embedded fluid sensors were fabricated entirely in-house. A list of all materials, supplies, and equipment used can be found in Appendix C. This process was initially adapted from softroboticstoolkit.org (Mengüç, n.d.), but modified and developed over the fabrication process. The final process is described following. A list of commonly-encountered issues, as well as the troubleshooting steps to avoid or alleviate them, can be found in Appendix B.

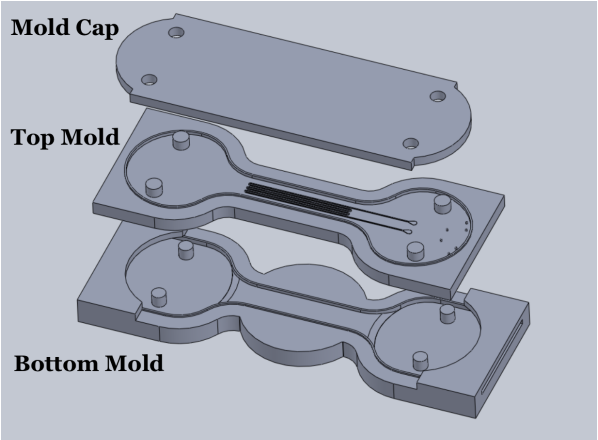

Figure 8: A breakdown of the mold's CAD model.

CAD solid models of three sensor mold components, taken from files available at softroboticstoolkit.org, were modified to the desired dimensions and 3D resin printed on a Formlabs Form 2 stereolithography printer. The molds were printed in a resin resistant to heat up to 80 C. The three mold components are shown and labelled in Figure 8.

Thirty grams of Ecoflex 00-30 were prepared by weighing equal parts of the two components, thoroughly blending by hand, and placing the mixing cup into a vacuum chamber until all bubbles were visually gone (5 minutes minimum). The top mold, bottom mold, and mold cap were sprayed with mold release, and pre-trimmed nylon fabric ends were inserted into the bottom mold. The silicone was then carefully poured into the bottom and top molds, ensuring laminar flow and absence of trapped air pockets. Silicone was poured until the molds were entirely filled, with surface tension holding some of the liquid above the level of the mold lip. There would be ~5-10 grams of excess silicone in the pour cup, but the larger mass was

required for even pouring. If there were any visible bubbles or trapped air at this stage, the molds were returned to the vacuum chamber for another 5 minutes before proceeding. The mold cap was carefully placed on the mold bottom, pressed from one side to the other to eliminate trapped air.

The molds were placed on a hot plate, preheated to 70 C along with a heavy stainless steel weight. The weight was placed atop the capped bottom mold, while the uncapped top mold simply rested on the hot plate. The molds were left to cure on the hot plate for ten minutes, removed, and left to air-cool to room temperature (approximately another ten minutes)(Figure 9).

The cap was carefully removed from the bottom mold, and the casting inspected for any trapped air. An additional 10 grams of EcoFlex 00-30 were prepared as above (or, if available, the remainder from the original cast was used). A very small amount was poured on the top surface of the bottom casting, and spread using the freshly-cut edge of a small sheet of acrylic transparency to form an even, thin layer. The open-faced mold was placed into a kiln preheated to 85 C for one minute to partially cure the thin layer.

Figure 9: silicone curing in mold

The top casting was demolded and laminated onto the bottom casting, still in its mold. The two layers were positioned by the pegs and alignment holes. The lamination should be done with extreme care to prevent obstruction of the internal channels, using tweezers to lay the top layer down from one side

progressively over to the other. With the two layers laminated, the complete sensor body was left to cure overnight (see Figure 10).

After fully cured, the sensor body was demolded in entirety. Two 27-gauge needle syringes were prepared: one with 1 mL of conductive fluid, one empty and fully depressed. Both needles were inserted into the sensor body at low angles until their tips had visibly entered the ends of the internal channels. By alternatingly evacuating air with the empty syringe, and injecting conductive fluid, the channels were filled until no air visibly remained within the sensor body.

Two short lengths of copper wire were prepared by stripping both ends to a length of ~8 mm. A wire end was plunged into each of the thin holes left by the syringe needles, until the stripped copper was observed to be within the channels and in contact with the conductive fluid. Silpoxy was applied liberally around the wire/sensor junction area to seal the system and fix the wire ends in place. Each sensor was tested with a multimeter to ensure electrical contact was extant. Finally, a pair of stainless steel eyes were sewn onto the undersides of the nylon fabric ends, completing the sensor.

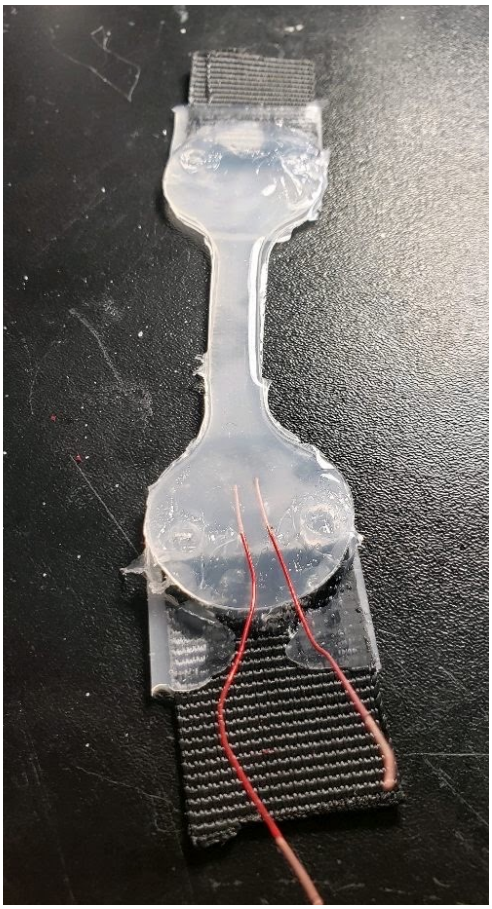

Figure 10: A completed sensor (KI-Gly)

The Electronics

Measuring the varying resistance of the flexible embedded fluid sensor is far easier with dedicated circuitry to clean up and amplify the signal. On its own, our sensor has resistances in

the millions of ohms, and across a 10cm stretch it can multiply that starting value by up to ten. This massive value and range makes it challenging to work with, so instead of using its actual value, we compare it to a reference resistance which resets the baseline. Unfortunately, in doing this we lose part of the range of the sensor, so the signal has to be amplified to get the output to an optimal range.

Design and Fabrication

The system we have developed is designed to balance the high sensitivity needed for the purpose, and the low sensitivity required to achieve good data outcomes. While much of this is true in the device's original state, it still requires some tweaking to get the readings to just the right range.

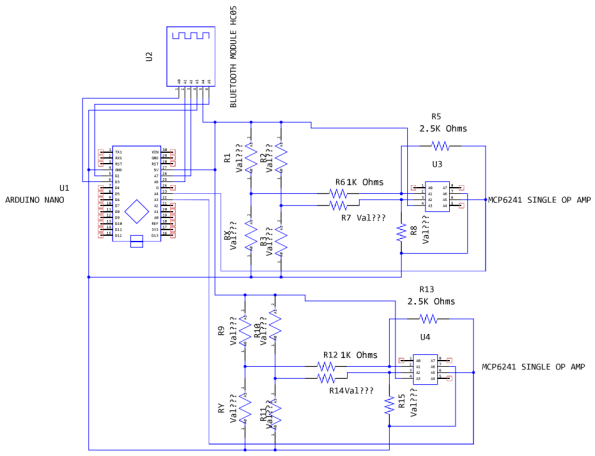

Figure 11: Schematic diagram of circuit to process sensor data

Our original design included passing the raw signal from the sensor through a wheatstone bridge and a non-inverting operational amplifier. The wheatstone bridge provided a relative reference of 7.8MΩ, which meant the resistance values we were examining were the difference between the real value and 7.8MΩ. The amplifier then took that difference and multiplied it by two so as to use the full 5V range of the arduino. These connections can be seen in Figure 11, though the final system used an operational amplifier solely for gain rather than as a traditional

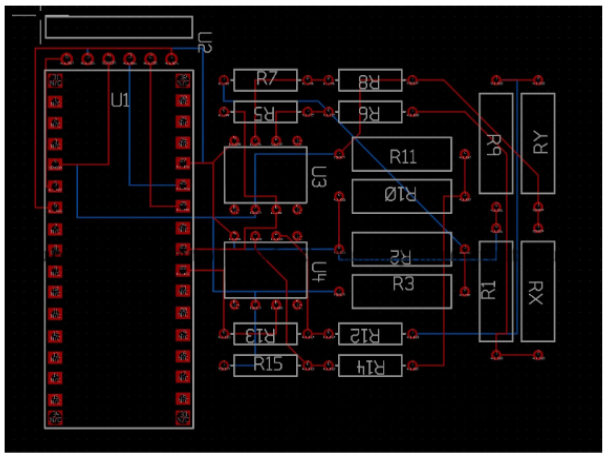

Figure 12: Laout of parts for printed circuit board

differential opamp, as the wheatstone bridge made that function more or less redundant.

To run the full system, we attached two sensors to two full wheatstone/op amp setups, which were both run off of a single central arduino nano. The nano has more processing power and ports than needed for this application, but it is a small, lightweight, standard module which was quick to prototype with and has extensive documentation online in case of problems. In a long term application, we would recommend a custom integrated circuit, but in this context the Nano was ideal. We also added a bluetooth transmission module, so that data could be wirelessly sent from the sensors to the computer. This circuit was developed into the schematic here, and a custom PCB was created with the assistance of the university laboratory (Figure 12).

The Harness

To ensure that the sensors and the electronics can be held in the appropriate positions on the user's back, we developed an unintrusive, reliable mounting mechanism. This mounting mechanism, inspired by climbing and parachuting harnesses, serves to ensure the ends of the sensors stay at their respective fixed points on the wearer's shoulders and back. Each strap of the harness is adjustable so the fixed points on a wide variety of body shapes and sizes without restricting their movement.

Constraints and Functional Specifications

The selected sensors will be mounted and located on the human body by means of a wearable harness. It must allow the sensors to measure the physiological responses of the superior and medial trapezius fiber groups. The harness serves as the interface between the soft

robotics sensors and the wearer's torso, while remaining safe under a normal variety of operating conditions. To maximize ease of use and minimize cost to researchers, the harness should be easy to apply and configure when compared to EMG, usable on a wide array of body types and sizes, and the initial capital cost to fabricate should be minimized.

The main ease-of-use functionality of the harness is the ability to non-invasively fix it to the participant without losing any of the measurement potential of the attached sensors. In order to do this, the harness must both minimize any impedance upon the wearer's natural motion, while also being adjustable such that it provides enough force to hold each end of the sensors to the desired locations on the body.

Muscle Measurements and Sensor Placement

In an attempt to minimize the number of sensors necessary to take the desired measurements, a common effective set of fixed points between the superior and medial fibres of the trapezius should be found. Given that the longest fibres of the superior trapezius are directly adjacent to those of the medial trapezius, a single set of effective fixed points can easily be found. One fixed point is between vertebra C-VII and T-I and the other will be at the Acromion process.

To determine the lengths of the sensors and how much they need to stretch, the backs of various individuals with different body types and sizes were measured. Each individual had the distance from their shoulders to their spine measured in five different positions: shoulders at rest, arms up as though on a computer at a desk, shoulders rolled back, shoulders rolled forward, and slouched posture. The maximum distance difference between individuals and the

maximum distance change for a single individual were used to determine what size the sensor needs to be.

Material Selection and Design

The difficulty in non-invasively taking the aforementioned measurements is ensuring the ends of the sensor stay at the fixed points on the body. The low friction between clothing and skin, and the elasticity of skin, muscle, and connective tissue create a barrier of uncertainty between the sensor and the skeleton. To reduce this uncertainty, friction between the fixed points and the skeleton must be maximized. To do this while remaining non-invasive, a chest harness compresses the ends of the sensors against the participant's clothing. The design for this harness was inspired by harnesses used in activities such as rock/mountain climbing and skydiving. Both of these disciplines have similar requirements for tightly fastening and locating hardware on the human body with minimal restriction of human motion. Therefore, they are appropriate starting points for a design that provides sufficient body coverage and compressive force to hold the fixed points firmly against their desired positions on the human participant's torso.

The structure of the harness is made of an elastic polyester fabric. The fabric's elasticity will minimize the restriction of the human participant's movement. It consists of eight straps: two on the chest, two on the back, one over and one under each arm. Each strap is individually adjustable to facilitate the original placement of the fixed points on the human participant's body and to maximize the participant's comfort. Strips of nylon provide stiff segments as junctions between straps and connectors for the sensors. A prototype (Figures 13 and 14) was initially completed to test this design and inform the design of the final harness.

Figure 13: The prototype harness.

Figure 14: The prototype harness on a person.

Harness Fabrication

The final harness design was made from elastic polyester fabric strapping connected adjustably at nylon anchor point assemblies, and fastened with buckles and ladder adjusters. It consists of two front-arm and two back-arm strapping assemblies, a front buckle assembly, two shoulder assemblies, and a back assembly. A more detailed, comprehensive account of this fabrication process can be found in Appendix D.

The lengths of elastic strapping were sewn from four layers of the polyester fabric, using cotton thread in a zig-zag stitch such that the stitching can stretch along with the strap.

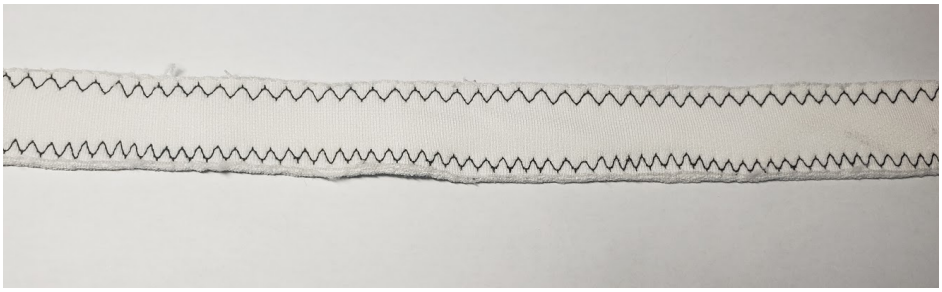

Figure 15: A harness strap with the zig-zag stitching.

The harness requires four 8” long, four 12” long, and two 16” long straps, which were then joined together with nylon reinforcement to form a pair of mirroring front-arm assemblies, and a pair of mirroring back-arm assemblies (Figure 15).

The shoulder assemblies are two of the four fixed points required by the design. They were made from three layers of nylon strap (for stiffness), ladder adjusters, and the hook elements of a hook-and-eye fastener pair. Likewise, the spine assembly locates the other two fixed points. It was made from ladder adjusters, hook elements, and five total layers of nylon strap (Figure 16).

Figure 16: The spine and shoulder assemblies with hooks attached

Once all components were made, all subassemblies were combined into the final harness. All adjustment locations and fixed points were tested for correct assembly orientation

(successful adjustability, fixed points facing away from body). The harness was then complete (Figure 17).

Figure 17: The fully-assembled harness on a human's back.

Testing the Device

The individual components of the device were tested to ensure they function as intended. This process was used to develop the design methodologies above (Methodology, The Harness and Methodology, The Sensor). For more in-depth view of the development processes, Appendix B for the sensor and Appendix D for the harness.

Sensor Testing

There are two main aspects of the sensors that must be tested to ensure their compliance with desired parameters: their functional range, and limits of failure. In order to take the measurements needed for this project, the sensors must have a resolution to pick up the movements produced by the slight contraction of the Trapezius. We must determine at what stretch range this resolution is achieved, and ensure that, when the sensor is in use at this stretch range, it does not mechanically fail.

Sensor Destructive Limit Testing. Two failed sensors that were not electrically functional, but otherwise mechanically sound, were stretched to destruction to determine their physical limits. One end of the sensor was fixed with a clamp, and stretched by hand alongside a meter stick. When the sensor failed, the final length and the location of failure was observed. Two sensors were stretched to the required functional strains and relaxed repeatedly for ten minutes to determine whether any damage due to fatigue or creep was visible.

Sensor Response over Functional Range. To determine sensor range and resistance, we took an electrically viable sensor (one with a complete and unbroken connection between the sensor leads) and measured the output voltage at different stretch lengths. To collect a reading, we set up the sensor as the second half of a simple voltage divider circuit,

which was read via Arduino Uno. In this setup, we stretched our sensor to discrete lengths, and recorded the voltage output measured. Using basic electrical math, we were able to calculate the resistance of the sensor at each length and derive a response curve. Both eGaIn and KI-Gly were tested in this way.

Harness Testing. To determine improvements for the final construction of the harness, it was put on a wide variety of body types. In doing so, the harness' longevity, fit, performance on various fabrics, and ease-of-use were tested. Any issues were noted, and the list of these issues were used to determine what needed changing when constructing the final version of the harness.

Results

Sensor Selection

Analysis of the background research indicated that the Flexible Embedded Fluid sensor family is the best option from the compiled list, followed by Smart Braids and Refraction Deformation/Optical sensors. Smart Braids were rejected for the high level of electrical complexity and requirements to obtain appropriate signals. Optical sensors were determined to be an overall attractive option, but prohibitively difficult to fabricate or obtain in the current context. Pneumatic deformation sensors simply do not measure the right physical phenomenon for our research. Dielectric elastomers were eliminated for both the inherent dangers of the required voltage and the relative challenges in fabricating or purchasing one. Flexible embedded fluid sensors are highly customizable in shape and size, can be fabricated in-house, and are overall best suited to complete an iterative design process within the scope of the project.

Device Testing

Sensor Functional Range.

	Rest	Desk	Shoulders Back	Shoulders Forward	Slouch
Small	12.70 | 13.01	12.63 | 12.95	10.68 | 11.54	12.88 | 13.29	12.64 | 13.23
Large	19.17 | 19.52	19.00 | 19.70	18.97 | 18.75	19.42 | 20.04	19.20 | 19.84

Table 3: Back Measurements from Various Body Types (Measurements in cm)

Table 3 above shows the data taken from measuring different individual's shoulders (see Section 2: The Device, Harness Design - Muscle Measurements and Sensor Placement). The longest the sensor would have to stretch, in order to accommodate both a small-shouldered individual and a large-shouldered individual, is 8.5cm (20.04cm-11.54cm). The most it would

have to stretch on a single person is 2.61cm (13.29cm-10.68cm). Based on this, it was determined to fabricare a sensor of 7.5cm in functional, unstretched length.

Sensor Destructive Limits. It was determined that the sensors could be repeatedly stretched, without damage, to a length of 30 cm; exceeding 300% total strain. Both sensors tested to destruction began to tear at the alignment holes past 32 and 34 cm total stretched length. The sensors tested with repeated cyclic strain/relaxation between fully relaxed and double the functional max length (15 cm total) showed no observable damage after approximately 600 cycles over ten minutes.

Sensor Electrical Response. The electrical response of each type of sensor was measured at 1cm, 2cm, 5cm, and 10cm stretch. Both sensors were equally electrically viable (unbroken, full wire) with the same approximate elastomeric composition, and the same unstretched length (7.5cm body length, measured between alignment holes). eGaIn generally operated around 2-8Ω, whereas KI-Gly operated between 7.8 and 74.5 Million Ω (see Figure 18).

	eGaIn Value			
cm	Bits (Min, Max)		VOut	Est. Ohms
0	1002	1007	4.91	1.79
1	999	1003	4.89	2.13
2	994	999	4.87	2.58
5	979	980	4.79	4.31
10	942	946	4.61	8.12

	KIGly Value			
cm	Bits (Min, Max)		VOut	Est. Ohms
0	114	117	0.56	7825714.00
1	85	88	0.42	10783283.24
2	62	64	0.31	15177142.86
5	29	32	0.15	32410819.67
10	12	15	0.07	74478666.67

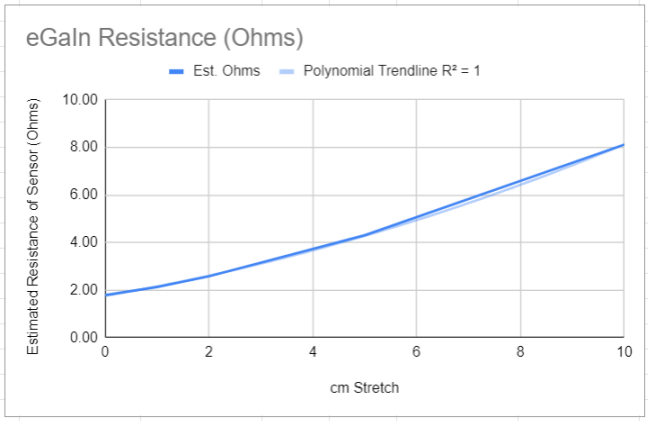

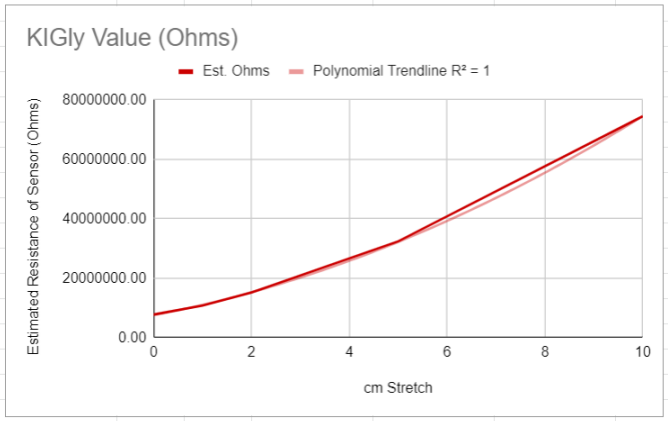

	eGaIn	KIGly
	y = p1*x^2 + p2*x + p3	y = p1*x^2 + p2*x + p3
	Coefficients:	Coefficients:
	p1 = 0.026372	p1 = 3.5249e+05
	p2 = 0.37313	p2 = 3.1716e+06
	p3 = 1.7571	p3 = 7.5527e+06
	Norm of residuals =	Norm of residuals =
	0.058607	4.63E+05

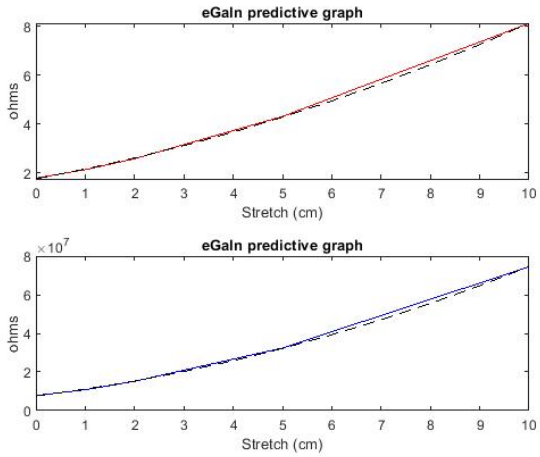

Figure 18 (top): The data taken for both the eGaIn and KI-Gly sensors at different stretch lengths

Figure 19 (bottom left): The low norm of residuals seen for each function expresses the quality of the data's fit to a parabolic curve.

Figure 20 (bottom right): Matlab-produced graphs modeling sensor behavior

After putting this data into Matlab, we were able to derive the order of the function and the polynomials. Both functions closely fit to parabolic curves, as can be seen in Figure 18. Predictive graphs, based on these models, of the stretch at any given length can be seen in Figure 19.

Harness Improvements. The main downfalls of the initial prototype were as follows: each strap was made far too long, and even after cutting some off and folding some of each strap over on itself, the triglide slide adjusters were unable to change the length of the straps as sufficiently as needed. Each strap was made only of a single layer of polyester fabric, and as such have a tendency to fray and not hold their shape, hindering stretch consistency and adjustability. The friction between the harness and most types of fabric was sufficient; nylon strips to add additional friction were unnecessary.

The final iteration has ladder slide adjusters so each individual strap can be tightened as far as needed, solving the problem of too much strap length. Each strap is made of four layers of polyester fabric, sewn together in such a way to prevent fraying. This helps each strap hold their shapes. In addition to adjusting to solve problems from the prototype, the final harness has only a single under-arm strap and no strips of nylon to increase friction. While not solving any issues the prototype faced, they simplify the manufacture of the harness and eliminate features that are of no use in the prototype.

Theoretical Calculations

To estimate how much a participant's trapezius muscles would have moved in reaction to a stimulus, we used data from a study which originally informed our own experimental design (Krantz et al., 2004). This study measured participant reactions via trapezius EMG to a Stroop Color Word test. The average experimental values for the group were reported as a percent of reference voluntary electrical contraction, which is equivalent to the maximum contraction of the trapezius muscle. Using preliminary data taken to determine optimal sensor size in this project, we were able to estimate that maximal contraction of the trapezius was between 1cm and 2cm, depending on the person. This allowed us to calculate the smallest distance in

centimeters we might expect a participant to express, which was 0.112cm (or 0.058cm, at -1 standard deviation)(see Tables 4 and 5).

TABLE 1

The summary effect of induced mental (Colour Word Test and Mental Arithmetic) and physical stress (Cold pressor test) on physiological measurements as compared with baseline measurements for women and men separately and for the total population, presented as means and standard deviations (SD). Significance test was performed with Analysis of variance (ANOVA) for repeated measurements; *Df*=1/10 (women); *Df*=1/9 (men); *Df*=1/20 (all). Two-tailed p-values.

	Women			Men			All		
Measurement	Exposure	Baseline	p	Exposure	Baseline	p	Exposure	Baseline	p
Blood pressure systolic (mm Hg)	139.5(24.2)	118.0(10.2)	0.005	139.6(11.2)	123.8(8.0)	0.0001	139.6(18.8)	120.8(9.4)	0.0001
Blood Pressure diastolic (mm Hg)	93.7 (14.8)	77.8 (11.2)	0.005	94.2 (8.1)	78.7 (8.0)	0.0001	93.9 (11.8)	78.3 (9.5)	0.0001
Heart rate (beats/min)	83.4 (10.4)	69.4 (9.1)	0.003	73.7 (6.3)	62.5 (9.0)	0.001	78.8 (9.9)	66.1 (9.5)	0.0001
Surface EMG (%RVE)	2.8 (7.0)	8.7 (5.9)	0.073	9.5 (3.7)	6.3 (3.4)	0.009	11.2 (5.8)	7.6 (4.9)	0.009
Epinephrine (pmol/min/kg.)	0.82 (0.35)	0.56 (0.36)	0.019	1.45 (0.65)	0.74(0.47)	0.0001	1.10 (0.59)	0.65(0.41)	0.0001
Norepinephrine (pmol/min/kg)	2.76 (1.04)	1.83 (0.67)	0.009	3.75 (0.94)	2.59(0.91)	0.002	3.20 (1.10)	2.17(0.85)	0.0001
Cortisol (nmol/l)	5.44 (1.63)	8.70 (7.46)	0.068	6.45 (2.34)	5.14(2.11)	0.075	5.92 (2.02)	7.00(5.76)	0.191

Maximal Contraction	shoulder width	maximal contraction	Exposure	Exp. St Dv
Person 1 (cm)	10	1	0.112	0.058
Person 3 (cm)	20	2	0.224	0.116

Table 4 (top): data from a previous study, which shows average EMG measurement over all participants under exposure condition as a percent RMV. Krantz, G., Forsman, M., & Lundberg, U. (2004). Retrieved from https://link-springer-com.ezpxy-web-p-u01.wpi.edu/content/pdf/10.1007/BF02734276.pdf

Table 5 (bottom): The participants we tested for our preliminary data with the smallest and largest shoulder widths showed different maximal contraction values, which translated into different amounts of trapezius movement under experimental conditions.

To determine device sensitivity, we simulated the filtering of our initial data and calculated the accuracy and noise of the system thereafter. Though we were not able to test the output of a single sensor with the circuit proposed previously, the mathematical models governing the output of any electrical system given an input are easily found. These models were applied to an early data set we took, which was derived simply from stretching the sensor and measuring the output in a voltage divider setup with respect to centimeters stretched. The outputs can be seen in Table 6 below.

Voltage Output vs cm Stretch	Est. Resistance (Ω)	VOut	VOut Wheatstone	Amplified (x2)
0	7825714.00	0.56	0.00411405	0.008228104009
1	10783283.24	0.42	0.40133963	0.8026792686
2	15177142.86	0.31	0.80266103	1.60532206
5	32410819.67	0.15	1.53011179	3.060223576
10	74478666.67	0.07	2.02600107	4.052002139

	0-1cm	5-10 cm
Volts/cm	0.7944511646	0.1983557127
cm/Volt	1.258730611	5.041447944
Noise (cm)	0.008811114278	0.03529013561

Table 6 (top): Centimeter stretch of the original sensor, the calculated resistance of the sensor at that stretch, and the voltage out after each stage of the filtering.

Table 7 (bottom): Using data from the final stage of filtering, both extremes of expected sensitivity were examined. Noise in centimeters was calculated off of the experimentally observed noise of 0.007V.

We discovered experimentally that the system has a noise level of plus or minus 1.4Bits, which is equivalent to 0.007 volts. We multiplied this by the distance we would have to stretch a sensor to get 1 volt, which gave us the noise in units of centimeters. The ranges shown here (0-1cm, and 5-10cm) are due to the nonlinearity of the device's sensitivity. Our intention, after preliminary testing, was to keep the device between a 0 and 10cm stretch, with an optimal prestrain at about 8cm of stretch. The data used for the final comparison was using the worst-case scenario of no stretch (0cm) and a participant one standard deviation smaller than

the smallest standard participant maximal movement. We found that we could read at a sensitivity of between 1.26 and 5.04cm/volt, yielding a noise of 0.009-0.035 cm (Table 7)

Cost Analysis

One of the primary objectives of this project was to increase the accessibility of psychophysiological studies by developing a device of a lower cost than the existing analogous too. To determine whether our developed device has the potential to be successful, a cost analysis was performed. Three different scenarios with associated final costs are shown below. The first estimates the costs incurred for an academic research team to fabricate a single copy of the device following the methodology described in this report. The second estimates the costs to have the required components custom fabricated by available, extant commercial vendors. The third scenario estimates the per-unit cost of a device fully brought to market and manufactured en mass.

Scenario 1. For a team of researchers, the cost to fabricate this device is effectively the combination of the necessary material costs, and the number of labor hours required to complete fabrication. It is assumed for this analysis that the researchers have access to all equipment used in the fabrication process. The total cost of a minimum order of materials to fabricate at least one harness and two sensors is $303.74 USD (see Appendix C for an itemized list with sources). The estimated total amount of labor to fabricate the harness is 40 hours, for a researcher unfamiliar with sewing. The estimated total time to fabricate two functional sensors is 20 hours (allowing for reasonable trial and error). Assuming a generous research stipend of $30,000/yr (PHDStipends, n.d.), converted to $15/hr, the required labor adds an additional $900 in cost, for a total of 300 + 900 = ~$1200.

Scenario 2. If a similar team of researchers were interested in a larger-scale study using ten copies of the device, it may instead make sense to outsource as much of the fabrication as possible, they may encounter the following. A freelance seamster/seamstress could be hired to fabricate the ten harnesses. Given their professional experience, and due to the process made more efficient by the economy of scale, it is estimated that ten harnesses could be fabricated in a 40-hour work week. At an hourly rate of $16/hr, (51-6052 Tailors, 2020) ten harnesses would cost 40 x 16 = $640, rounded to $700. Similarly, a prop-maker could be commissioned to cast and laminate twenty sensor bodies, at a roughly estimated cost of $1000. The researchers would then have to inject conductive fluid and finish each sensor, and do final assembly of the devices, for an estimated 40 hours ($600). Electronics still need to be purchased, at a cost of $38.19 per device, as per Appendix C. In total, outsourcing as much work as possible, ten complete devices could be fabricated for 700 + 1000 + 600 + 380 = $2680, or $268 per device. However, it should be expected that some additional work and expense may be incurred by prototyping/communicating with the outside vendors.

Scenario 3. If the device were brought to market through dedicated manufacturing, the economies of scale allow for the utilization of much more efficient fabrication processes. In an industrial setting, a manufacturing cell of the same skilled seamsters and seamstresses could rapidly produce the harness. To determine a per-unit retail cost, a good analog would be a chest harness for rock climbing. The average price of some common models is $60 USD (Buy OPG Seat, n.d., CMI Adjustable Chest Harness, n.d., Petzl Voltige, n.d.). Likewise, closed-die injection molding can rapidly produce sensor components at costs of a simple multiple of the material cost (How Much Does, 2020), such that a pair of sensor bodies would cost less than $10 USD. Injection of conductive fluid and assembly of electronics are also processes capable of good precision and low cost in an industrial manufacturing environment. A reasonable analog would

be a commercially available data acquisition system/data logger with onboard storage, many of which are available in the $100 USD price range. In total, a manufactured product version of the device might retail for 60 + 10 + 100 = 170 USD.

A summary of these three scenarios is shown in Table 8 below.

	Scenario 1	Scenario 2	Scenario 3
Details	Single device, fabricated in-house	Ten devices, labor outsourced	Device commercially manufactured
Per-unit cost	$1200	$268	$170

Table 8: Summary of cost analysis with different manufacturing methods

Discussion

The results we were able to obtain helped inform our understanding of how a device like this should be optimally constructed, as well as guide us towards conclusions on its effectiveness. This analysis consisted of electrical analysis to find the ideal conductive liquid and design corresponding circuitry, destructive and nondestructive testing of the sensors to determine working ranges, and a mathematical exploration of overall sensor effectiveness. To examine the device's financial accessibility, we conducted a cost analysis. Without a full study, analysis of the devices' ease-of-use was limited to the researchers' experience.

In regards to the selection of a conductive fluid for the sensors, both eGaIn and KI-Gly were found to have associated benefits and drawbacks. The dramatic difference in resistance ranges between the eGaIn-filled sensors and the KI-Gly-filled sensors had significant implications for the appropriate uses for each. While both sensors showed similar response curves, the massive value range of the KI-Gly made it appealing for this application, as a tiny change in distance stretched amounted to a massive change in resistance value. This makes it incredibly easy to read, and keeps current low, making it safer for participants in case of electrical malfunction.

The results of our KI-Gly-based mathematical analysis of sensitivity suggest that the sensor fabricated would have been accurate enough to measure experimental changes in trapezius strain. This assertion is based on the idea that the system noise is lower than the smallest unit of strain we could want to measure. Without conducting experimental testing, however, it is difficult to say if this device would have been a significant improvement over EMG in a research context. The noise experienced by EMG sensors is influenced by a multitude of factors, including the stability of the attachment site, participant sweat levels, relationship of the

sensor's placement to the location of the heart, and more (Chowdhury, 2013). As such, we have not found a good way to estimate hypothetical expected EMG noise level to compare our data to. All we can say with this testing is that it theoretically would have worked as a replacement to EMG in this application.

When comparing the cost between EMG and our sensor, there is no question that the sensor developed as a result of this project is more financially accessible. While a set of Delsys EMG sensors can be purchased for $20,000, our device at worst would cost $1200 if fabricated in-house, and at best would cost $170 if produced on a large scale through commercial manufacturing. At worst, our device is an order of magnitude less expensive than current devices.

It is important to recognize the effect of the COVID-19's crisis's timing in our project. The most evident challenge to this project's viability is that we were not able to do a full-scale experimental study on real participants. Such a study was planned within the scope of this project, and the full experimental design can be found in Appendix E. Unfortunately, the experiment we designed was scheduled to be run in March of 2020, which marked the beginning of the Boston area's COVID-19 response. The institution at which this study would have been run, amongst others, ceased all in-person interactions for the remainder of the academic year.

Without completing the study, we cannot address with experimental data how our device would have compared to traditional EMG, either in functionality or ease-of-use. Ideally, this study would have been run on a large number of participants of a variety of body types and shoulder sizes. Participants would have worn both the device developed by this project, and the EMG sensors, to allow for direct comparison. Participants would have performed a maximal contraction/relaxation test to get a baseline, before engaging in a variety of stress tests as

described in Appendix E. Data would have been analyzed for each participant comparing the noise level of the EMG with the noise level of the flexible embedded fluid sensor. This comparison would show to what degree our sensor device was A. able to measure trapezius movement, B. comparable in reading to EMG sensors in experimental conditions, and C. able to measure stress.

Instead, one of our only options was to complete a mathematical analysis of the sensors' capabilities. While the math suggests that our device would have worked, it relies on the idea that our harness works effectively, and that the sensor does actually measure the movement occurring in the trapezius muscle. Our calculations, by nature, have to make the jump from muscular movement to sensor stretch assuming a direct and complete relationship, when in reality this transfer is likely to be imperfect.

We would also like to acknowledge the limitations to this study's external validity. While flexible embedded fluid sensors have demonstrated usefulness in measuring trapezius movement, they do not precisely replicate what EMG does. Because EMG actually detects the electrical impulses moving through muscles, it can measure much smaller changes than a strain sensor of any kind ever could. At the moment, soft sensors have no capacity to replicate this technology. This means that while this device may currently function for some applications of psychophysiology, the analysis of small muscle groups would require the development of strain sensors smaller by at least an order of magnitude than those currently studied.

Conclusions

Psychophysiology is a budding field with massive potential to create opportunities and foster scientific progress. Being able to have more tools to support data-driven experimentation benefits the research community. To ensure that this technology is available to as many people as possible, our study aimed to increase accessibility to psychophysiological tools. By developing a soft robotic sensor for the application of measuring trapezius movement as a reflection of participant stress, we explored alternatives for technology which is currently prohibitively expensive or challenging to use.

Our mathematical models suggested that a KI-Gly-based sensor would have been capable of measuring the movement of the trapezius under experimental conditions, given that the harness successfully secured the sensor to the fixed points on the participant. In terms of affordability and manufacturability, this device would be incredibly affordable (less than $200, as compared to EMG's $20,000) if the product were brought to market and manufactured commercially. For a set of researchers to fabricate, it takes significantly more money, time, and expertise.

As previously noted, an experimental study was planned for the original scope of this project. Since it was not possible to do so, the most obvious extension of this project would now be to actually perform a stress study using both the device manufactured and EMG. The study we conceived of is described in our Discussion, with a more detailed background in Appendix E. While this proposal forms a good basis, we would encourage the study described to be conducted with additional psychophysiological measures or surveys to corroborate participant stress levels. Our study was designed to focus on the direct comparison of the two sensors simply because of the time and resources available to us, but a larger study could conduct a

more thorough investigation of device validity. To further assess the accessibility of the device, we would also recommend adding a survey for both experimenters and participants inquiring about ease of use and comfort level.

While these technologies were explored primarily for research processes, there is also significant opportunity here for entrepreneurial endeavors. In a world increasingly motivated by data, tools such as smartwatches which help people monitor their own physiological or psychological statuses represent a significant market segment. Biosensors are also popular in fields such as sports medicine, physical therapy, and rehabilitation science. The device developed by this project has the potential for a variety of applications in these fields, anywhere that precise, high-resolution, and non-invasive measuring of body movement is useful. Devices like this may aid medical professionals in making diagnoses, and/or help patients along their path to recovery. Regardless of the application, we hope that the research and methods presented in this study contribute to the advancement of the fields of soft robotics and psychophysiology, and we encourage others to pursue interdisciplinary research of this type.

References

Allen, A. P., Kennedy, P. J., Cryan, J. F., Dinan, T. G., & Clarke, G. (2014). Biological and psychological markers of stress in humans: Focus on the Trier Social Stress Test. *Neuroscience & Biobehavioral Reviews*, *38*, 94–124. doi: 10.1016/j.neubiorev.2013.11.005

Benning, S. D., & Oumeziane, B. A. (2017). Reduced positive emotion and underarousal are uniquely associated with subclinical depression symptoms: Evidence from psychophysiology, self-report, and symptom clusters. *Psychophysiology*, *54*(7), 1010–1030. doi: 10.1111/psyp.12853 https://onlinelibrary-wiley-com.ezpxy-web-p-u01.wpi.edu/doi/full/10.1111/psyp.12853

"Buy OPG Seat Climbing Caving Harness with Half-Moon Screw Link." *Omniprogear*, www.omniprogear.com/OPG-p/OPG_SHNC.htm?gclid=Cj0KCQjw2PP1BRCiARIsAEqv-pQfjFU6DePwEmnBpoAaTe9e0Q8UjrTKBCAlNgr3_HnZmI0HSTaJUnAaAksbEALw_wcB.

Chowdhury, R., Reaz, M., Ali, M., Bakar, A., Chellappan, K., & Chang, T. (2013). Surface Electromyography Signal Processing and Classification Techniques. *Sensors,13*(9), 12431-12466. doi:10.3390/s130912431

Daily Life. (2019, November 1). Retrieved November 10, 2019, from https://www.stress.org/daily-life.

"CMI Adjustable Chest Harness - #HAR5." *Westech Rigging Supply - Rigging Equipment,*

Rigging Hardware, Tree Gear & Logging Supplies, www.westechrigging.com/cmi-chest-harness.html?gclid=Cj0KCQjw2PP1BRCiARIsAEqv-pTYRZYv6eppWGAR4DAQ54-U6tgV---z4Wy29tzjPkhxvAt6_97EKD8aAkQREALw_wcB.

Farnsworth, B., Ph.D. (2019, February 18). What is EMG (Electromyography) and how does it work? Retrieved March 8, 2019, from https://imotions.com/blog/electromyography-101/

Gorman, N., MSc. (2020). Trapezius muscle. Kenhub. https://www.kenhub.com/en/library/anatomy/trapezius-muscle

Henze, G.-I., Zänkert, S., Urschler, D. F., Hiltl, T. J., Kudielka, B. M., Pruessner, J. C., & Wüst, S. (2017). Testing the ecological validity of the Trier Social Stress Test: Association with real-life exam stress. Psychoneuroendocrinology, 75, 52–55. doi: 10.1016/j.psyneuen.2016.10.002

"How Much Does Injection Molding Cost?: Rex Plastics Mold Manufacturer." *Rex Plastics*, 9 Jan. 2020, rexplastics.com/plastic-injection-molds/how-much-do-plastic-injection-molds-cost.

Hoehn-Saric, Rudolf. "Somatic Manifestations in Women With Generalized Anxiety Disorder." *Archives of General Psychiatry*, vol. 46, no. 12, Jan. 1989, p. 1113., doi:10.1001/archpsyc.1989.01810120055009.

Krantz, G., Forsman, M., & Lundberg, U. (2004). Consistency in physiological stress responses and electromyographic activity during induced stress exposure in women and men. *Integrative Physiological & Behavioral Science*, *39*(2), 105–118. doi: 10.1007/bf02734276

Larsson, S.-E., Larsson, R., Zhang, Q., Cai, H., & Berg, P. K. (1995). Effects of psychophysiological stress on trapezius muscles blood flow and electromyography during static load. *European Journal of Applied Physiology and Occupational Physiology*, *71*(6), 493–498. doi: 10.1007/bf00238550

Lundberg, U. (1999). Coping with stress: neuroendocrine reactions and implications for health. *Noise and Health*, *1*(4). Retrieved from https://go-gale-com.ezproxy.wpi.edu/ps/i.do?id=GALE|A164864469&v=2.1&u=mlin_c_worpoly&it=r&p=AONE&sw=w

Lundberg, U., Kadefors, R., Melin, B., Palmerud, G., Hassmén, P., Engström, M., & Dohns, I. E. (1994). Psychophysiological stress and emg activity of the trapezius muscle. *International Journal of Behavioral Medicine*, *1*(4), 354–370. doi: 10.1207/s15327558ijbm0104_5

"Petzl Voltige." *Backcountrygear.com*, www.backcountrygear.com/voltige.html?gclid=Cj0KCQjw2PP1BRCiARIsAEqv-pSdMFH6vAY-B9uN5RohGDDWhULz_sBZx3rsi_AxKmtKN25mNr1v1l0aAqXjEALw_wcB.

Pizzolato, S., Tagliapietra, L., Cognolato, M., Reggiani, M., Müller, H., & Atzori, M. (2017). Comparison of six electromyography acquisition setups on hand movement classification tasks. *Plos One*, *12*(10). doi: 10.1371/journal.pone.0186132

"PHD Stipends." *PhD Stipends*, www.phdstipends.com/.

Rash, G. S., EdD. (n.d.). Electromyography Fundamentals. Retrieved March 5, 2019, from http://myweb.wwu.edu/~chalmers/EMGfundamentals.pdf

Schleifer, L. M., Spalding, T. W., Kerick, S. E., Cram, J. R., Ley, R., & Hatfield, B. D. (2008).

Mental stress and trapezius muscle activation under psychomotor challenge: A focus on EMG gaps during computer work. *Psychophysiology*, *45*(3), 356–365. doi: 10.1111/j.1469-8986.2008.00645.x

Sensors. (n.d.). Retrieved March 5, 2019, from https://softroboticstoolkit.com/sensors

Stress relief is within reach. (2019). Retrieved November 10, 2019, from https://softroboticstoolkit.com/sensors

"Ecoflex™ 00-30 Product Information." *Smooth-On*, www.smooth-on.com/products/ecoflex-00-30/.

Subbu, R., Weiler, R., & Whyte, G. (2015). The practical use of surface electromyography during running: Does the evidence support the hype? A narrative review. *BMJ Open Sport & Exercise Medicine,1*(1). doi:10.1136/bmjsem-2015-000026

"51-6052 Tailors, Dressmakers, and Custom Sewers." *U.S. Bureau of Labor Statistics*, U.S. Bureau of Labor Statistics, 31 Mar. 2020, www.bls.gov/oes/current/oes516052.htm.

Vanman, E. J., Saltz, J. L., Nathan, L. R., & Warren, J. A. (2004). Racial Discrimination by Low-Prejudiced Whites: Facial Movements as Implicit Measures of Attitudes Related to Behavior. *Psychological Science*, *15*(11), 711–714. doi: 10.1111/j.0956-7976.2004.00746.x

Vrana, S. R. (1993). The psychophysiology of disgust: Differentiating negative emotional contexts with facial EMG. *Psychophysiology,30*(3), 279-286. doi:10.1111/j.1469-8986.1993.tb03354.x

Wijsman, J., Grundlehner, B., Penders, J., & Hermens, H. (2013). Trapezius muscle EMG as predictor of mental stress. *Wireless Health 2010 on - WH 10*, *12*(4). doi: 10.1145/1921081.1921100

Argosy Publishing (n.d.). *Trapezius*. Retrieved from https://cervicalspine.wordpress.com/anatomy/myology

Please see Appendix A for additional resources.

Appendix A: Resource Compendium

Resources not explicitly referenced, but used to inform this study.

Psychophysiology: Exploration of constructs and measures

Lundberg, Ulf, et al. "Psychophysiological Stress and Emg Activity of the Trapezius Muscle." *International Journal of Behavioral Medicine*, vol. 1, no. 4, 1994, pp. 354–370., doi:10.1207/s15327558ijbm0104_5. https://link.springer.com/article/10.1207/s15327558ijbm0104_5

- Blood Pressure
- Heart Rate
- Urinary Catecholamines
- Salivary Cortisol
- Self-Report
- Trapezius EMG
- Stress

Lundberg, Ulf, et al. "Psychophysiological Stress Responses, Muscle Tension, and Neck and Shoulder Pain among Supermarket Cashiers." *Journal of Occupational Health Psychology*, vol. 4, no. 3, 1999, pp. 245–255., doi:10.1037/1076-8998.4.3.245. https://psycnet.apa.org/buy/1999-05612-006

- Blood Pressure
- Heart Rate
- Urinary Catecholamines
- Trapezius EMG
- Stress

Flor, Herta, et al. "Assessment of Stress-Related Psychophysiological Reactions in Chronic Back

Pain Patients." *Journal of Consulting and Clinical Psychology*, vol. 53, no. 3, 1985, pp. 354–364., doi:10.1037/0022-006x.53.3.354.

https://psycnet.apa.org/record/1985-25818-001

- Heart Rate
- GSR
- Paraspinal EMG
- Frontalis EMG
- Stress
- Depression

Westerink, Joyce H. D. M., et al. "Computing Emotion Awareness Through Galvanic Skin Response and Facial Electromyography." *Probing Experience Philips Research*, 2008, pp. 149–162., doi:10.1007/978-1-4020-6593-4_14.

https://link.springer.com/chapter/10.1007/978-1-4020-6593-4_14

- GSR
- Zygomaticus Major EMG
- Corrugator Supercilii EMG
- Frontalis EMG
- Valence

Larsson, Sven-Erik, et al. "Effects of Psychophysiological Stress on Trapezius Muscles Blood Flow and Electromyography during Static Load." *European Journal of Applied Physiology and Occupational Physiology*, vol. 71, no. 6, 1995, pp. 493–498., doi:10.1007/bf00238550.

https://link.springer.com/article/10.1007/BF00238550

- Laser-Doppler Flowmetry
- Trapezius EMG
- Stress

Zhai, Jing, et al. "Realization of Stress Detection Using Psychophysiological Signals for

Improvement of Human-Computer Interaction." *Proceedings. IEEE SoutheastCon, 2005.*, doi:10.1109/secon.2005.1423280.

https://ieeexplore.ieee.org/abstract/document/1423280

- Blood Volume Pulse (Blood Pressure)
- Pupil Dilation
- GSR
- Stress

Hoehn-Saric, Rudolf. "Somatic Manifestations in Women With Generalized Anxiety Disorder." *Archives of General Psychiatry*, vol. 46, no. 12, Jan. 1989, p. 1113., doi:10.1001/archpsyc.1989.01810120055009.

https://jamanetwork.com/journals/jamapsychiatry/article-abstract/494797

- Forehead EMG
- Gastrocnemius EMG
- GSR
- Heart Rate
- Anxiety

Vrana, Scott R. "The Psychophysiology of Disgust: Differentiating Negative Emotional Contexts with Facial EMG." *Psychophysiology*, vol. 30, no. 3, 1993, pp. 279–286., doi:10.1111/j.1469-8986.1993.tb03354.x.

https://www.ncbi.nlm.nih.gov/pubmed/8497557

- Levator Labii EMG -> Disgust
- Corrugator EMG -> Negative
- Zygomatic EMG -> Joy
- Heart Rate -> Disgust, Anger, Joy (vs Pleasantness)

- GSR

Benning, S. D., & Oumeziane, B. A. (2017). Reduced positive emotion and underarousal are uniquely associated with subclinical depression symptoms: Evidence from psychophysiology, self-report, and symptom clusters. *Psychophysiology*, *54*(7), 1010–1030. doi: 10.1111/psyp.12853 https://onlinelibrary-wiley-com.ezpxy-web-p-u01.wpi.edu/doi/full/10.1111/psyp.12853

- Postauricular EMG
- GSR/SCR
- EEG
- LPP (Lateral Positive Potential) Amplitude (Startle Blink?)
- Corrugator EMG
- Zygomatic EMG
- Depression

Lang, Peter J., et al. "Emotion, Motivation, and Anxiety: Brain Mechanisms and Psychophysiology." *Biological Psychiatry*, vol. 44, no. 12, 1998, pp. 1248–1263., doi:10.1016/s0006-3223(98)00275-3. https://www.sciencedirect.com/science/article/abs/pii/S0006322398002753

- Corrugator EMG
- Zygomatic EMG
- Heart Rate
- GSR
- Cortical ERP (EEG)
- Pleasure/Arousal Valence

Hodges, William F. *Emotions and Anxiety (Ple: Emotion): New Concepts, Methods, and*

Applications. Taylor & Francis Ltd, 2015, https://books.google.com/books?hl=en&lr=&id=8JjlCAAAQBAJ&oi=fnd&pg=PA175&dq=psychophysiology&ots=5SYqIqor-N&sig=00wNCjHDmSbtbUeueq6Q2TwK2TA#v=onepage&q=psychophysiology&f=false.

Page 184

- GSR
- Heart Rate

Willmann, Magali, and Benoît Bolmont. "The Trapezius Muscle Uniquely Lacks Adaptive Process in Response to a Repeated Moderate Cognitive Stressor." *Neuroscience Letters*, vol. 506, no. 1, 2012, pp. 166–169., doi:10.1016/j.neulet.2011.10.073. https://www.sciencedirect.com/science/article/abs/pii/S0304394011014856

- Flexor Pollicis Brevis EMG
- Biceps Brachii EMG
- Triceps Brachii EMG
- Trapezius EMG
- Gastrocnemius EMG
- Soleus EMG
- Stress

Wijsman, Jacqueline, et al. "Trapezius Muscle EMG as Predictor of Mental Stress." *Wireless Health 2010 on - WH 10*, 2010, doi:10.1145/1921081.1921100. https://dl.acm.org/doi/10.1145/2485984.2485987

- Trapezius EMG
- Stress

Soft Robotics

Sensors. (n.d.). Retrieved March 5, 2019, from https://softroboticstoolkit.com/sensors

Stress relief is within reach. (2019). Retrieved November 10, 2019, from

The Soft Robotics toolkit is an overview of the dominant technologies in the soft robotics field today, and contains comprehensive guides on the function and form of each sensor type. We found the design for the sensor we ended up developing on this website, and we are very grateful for the 3D models, instructions, and tips they provided. Our development of our sensor builds on information found here.

"Soft and Stretchy Fabric-Based Sensors for Wearable Robots." Wyss Institute, 13 July 2017, wyss.harvard.edu/news/soft-and-stretchy-fabric-based-sensors-for-wearable-robots/.

Carey, S. (2019). Survey of Soft Robotic Sensors [Unpublished manuscript]. Worcester Polytechnic Institute.

Survey of Soft Robotic Sensors

This survey of soft robotics technology was conducted previously by one of the authors of this paper, and includes a large set of soft robotics resources. This paper and the summaries it presents were used informally to guide our sensor choice.

Appendix B: Fabrication of Flexible Embedded Fluid Sensor

Iterative Design Process

The development of the final flexible embedded fluid sensor involved multiple design and process iterations. Some particularly noteworthy improvements are listed following.

1. Increased silicone volume in the pour cup allowed for laminar flow when casting, eliminating air bubbles and the requirement for a second vacuum stage.
2. Top mold cured without a mold cap, reducing trapped air and cast failure rate.
3. Mold cap of bottom mold pre-wetted with silicone layer, reducing trapped air and cast failure rate
4. Molds cured on a hot plate instead of in a kiln, increasing heat transfer rate and improving cure time and consistency.
5. Adhesive layer of silicone partially cured under higher temperature to better consistency.
6. Silpoxy used to fill alignment holes to increase lamination strength.

Common Failures and Troubleshooting

Issue / Mode of Failure	Troubleshooting Steps
Air bubbles in silicone cast, pre-cure	Increase time under vacuum
Air bubbles in silicone cast, post-cure	Attempt to reduce trapped air by increasing pre-wetting of the mold cap, and applying less pressure when initially capping molds.
Channels obstructed after lamination	Increase adhesive layer partial cure time
Layers delaminate during injection	Decrease adhesive layer partial cure time, reduce injection speed of fluid, increase the use of second syringe to evacuate air and create negative pressure in channels
Silicone tears from nylon ends	Reduce amount of mold release used in ends of bottom mold

Appendix C: List of Supplies, Materials, and Equipment

Sensor Development

Materials			
Material	**Source**	**Cost of Material Needed to Make one Sensor**	**Minimum Cost to Buy**
Elastomeric Substrate (Ecoflex 00-30 or similar)	https://shop.smooth-on.com/ecoflex-00-30	$1.68/30g	$25.36/1lb
Silpoxy Silicone adhesive	https://www.walmart.com/ip/Sil-Poxy-Silicone-Adhesive-3-Ounce-Tube/605621549?wmlspartner=wlpa&selectedSellerId=3676	$0.40/1g	$36.63/3 oz
Hook and Eye Clasps	https://www.amazon.com/Honbay-Silver-Closures-Sewing-Clothing/dp/B07F8PNYBX/ref=sr_1_3?dchild=1&keywords=hook+and+eye+silver&qid=1587488522&sr=8-3	$0.40	$8.99 for 100
eGaIn	https://www.sigmaaldrich.com/catalog/product/aldrich/495425?lang=en&region=US	$15.70/1g	$78.50/5g
Potassium Iodide (KI)	https://www.sigmaaldrich.com/catalog/product/sigald/207969?lang=en&region=US	$0.50/1g	$49.80/100 g
Glycerol	https://www.sigmaaldrich.com/catalog/product/sigma/49781?lang=en&region=US	$0.11/1mL	$56.70/500 mL
27 gauge needles and syringes	https://www.healthwarehouse.com/-205590.html	$0.90	$8.99/10 units
Electrical wire (small gauge)	https://www.remingtonindustries.com/magnet-wire/magnet-wire-26-awg-enameled-copper-8-spool-sizes/?gclid=Cj0KCQjw2PP1BRCiARIsAEqv-pSeevJTRQ4VAU_6Gx1fnhwItVyH6xEcQNBROSzmCpmLsKl4_haN6HEaAmTeEALw_wcB	$0.02/5in	$7.16/160ft

	Totals:	$3.11 for a single KI-Gly sensor	$193.64 for a minimum order

Supplies and Equipment	
Item	**Notes**
3D Stereolithographic resin printer	Used: Formlabs Form 2
Vacuum Chamber	Capable of fitting pour cups, molds
Hot Plate	Capable of holding 70 C
Kiln or Oven	Capable of holding 80 C
Pour cups, stir rods, paper towels, isopropyl alcohol	Supplies for preparing and cleaning silicone
Mold Release	WD-40
Craft knife	For demolding
Acrylic transparency	For flattening adhesive layer

Harness Development

Material	Source	Cost of Material Needed to Make one Harness	Minimum Cost to Buy
Elastic Polyester Fabric	https://www.moodfabrics.com/black-antibacterial-and-wicking-polyester-jersey-316096	$2.50	$20.00/yard
Nylon Strap Webbing	https://www.amazon.com/Strapworks-Military-Spec-Nylon-Webbing/dp/B07J39J3X6/ref=sr_1_8?dchild=1&keywords=nylon+webbing+1+inch&qid=1587487996&sr=8-8	$2.00	$11.40/reme
Hook and Eye Clasps	https://www.amazon.com/Honbay-Silver-Closures-Sewing-Clothing/dp/B07F8PNYBX/ref=sr_1_3?dchild=1&keywords=hook+and+eye+silver&qid=1587488522&sr=8-3	$0.40	$8.99 for 100
Cotton Thread	https://www.joann.com/gutermann-natural-cotton-thread-solids-876-yd/xprd1130586.html	$0.04	$8.49/876yd
Plastic Slider Clips	https://www.amazon.com/YGDZ-Release-Plastic-Buckles-Black/dp/B074MPHS4N/ref=sr_1_9?dchild=1&keywords=plastic+buckles+BTNOW+1+inch&qid=1587488866&sr=8-9	$0.40	$10.99 for 30
Ladder Adjusters	https://www.amazon.com/gp/product/B075ZQH9LS/ref=ppx_yo_dt_b_asin_title_o09_s00?ie=UTF8&psc=1	$6.60	$8 for 12
	Totals:	$11.94 for a single harness	$67.89 for a minimum order

Equipment Required: Sewing machine

Electrical

Equipment Required: Access to PCB Printer (can be substituted for order-online), Soldering iron and solder, Multimeter, Computer for processing and storing information

For Testing: Solderless Breadboard and respective wires

Material	**Source**	**Cost of Material Needed to Make one Board supporting 2 Sensors**	**Minimum Cost to Buy**
Arduino Nano	https://store.arduino.cc/usa/arduino-nano	$22.00	$22.00 for 1
7.8MΩ resistors	https://www.amazon.com/LeaningTech-HC-05-Module-Pass-Through-Communication/dp/B00INWZRNC	$4.32	$0.54 for 1
Resistors of any value in a 1:2 ratio	https://www.mouser.com/ProductDetail/Welwyn-Components-TT-Electronics/MFP2-100RJI?qs=sGAEpiMZZMsPqMdJzcrNwjc%252B2yVpPxPiexLwKUh2E2g%3D	$0.12	$0.12 for 1
Operational amplifiers	https://www.mouser.com/ProductDetail/Microchip-Technology/MCP6241-E-P?qs=sGAEpiMZZMtOXy69nW9rM%2FUd2%252By9j2EZj7uWZoLIFk0%3D	$0.30	$0.30 for 1
Batteries (at least 5V)	https://www.digikey.com/product-detail/en/panasonic-bsg/6LF22XWA-B/P687-ND/5067196	$1.50	$1.50 for 1
Battery caps	https://www.digikey.com/product-detail/en/keystone-electronics/232/36-232-ND/303804	$0.48	$0.48 for 1
Bluetooth transmitter	https://www.amazon.com/LeaningTech-HC-05-Module-Pass-Through-Communication/dp/B00INWZRNC	$8.49	$8.49 for 1
Printed Circuit Board	https://www.pcbway.com/	$1	5 for $5
	Totals:	$38.19 for a single device	$42.21 for a minimum order

Appendix D: In-depth Assembly Instructions for the Harness

The final harness consists of four 8” long, four 12” long, and two 16” long straps, each made of four layers of elastic polyester. For each strap, four pieces of fabric must be cut. Each piece must be one and a half inches wide by the length of the given strap with two inches extra on the ends. When four strips of fabric are cut to length, they should be pinned together along either of the short edges. Guidelines must be drawn ⅛” and ¼” in from the long sides of the top strip. The line at ⅛” defines where the edge of the final strap will be and the ¼” line is a guide for the sewing machine. Pin the four strips of fabric together such that they are firmly fastened to each other but the sewing machine foot can follow the ¼” line. Using a ¼” zig-zag stitch and cotton thread, stitch the four strips of fabric together along the ¼” line on both sides. Once this is completed, use a simple straight stitch along the lines at either end of the strap. When all sewing is completed, cut along the ⅛” line, making sure to not cut the stitches, to reduce the strap to its final width. Cut along the straight stitch, again ensuring it is not cut, to reduce the strap to its final size and eliminate the last of the excess fabric.

When all straps are sewn together and trimmed, it is time for assembly. Two 1”, two 2”, two 3”, three 5.5”, and one 9” strips of nylon must be cut for use as connectors. The 2” strips must be folded in half and used to connect the clip to two ladder adjusters. This forms the buckle assembly (Figures 15 and 16).

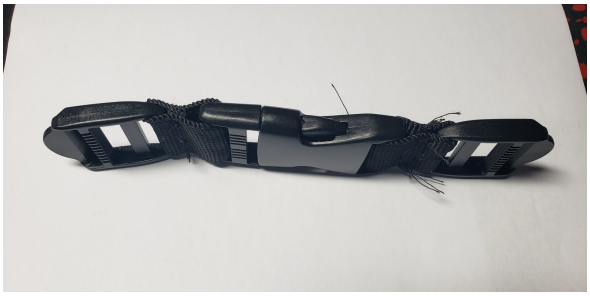

Figures 15 (Left): The buckle assembly, viewed from the front.
Figure 16 (Right): The buckle assembly, viewed from the top.

Two of the 5.5” strips must be tri-folded and sewn together to connect two ladder adjusters. This forms the shoulder assemblies (Figures 17 and 18).


Figure 17 (Left): The Shoulder Assemblies, viewed from the top.
Figure 18 (Right): The Shoulder Assemblies, viewed from the side.

The 9” strip must be bi-folded and sewn to form a double-layer, 4.5” strip of nylon. The final 5.5” strip must be tri-folded and used to connect two additional ladder adjusters with the 4.5” double layer nylon sewn in the middle. This forms the spine assembly (Figures 19 and 20).

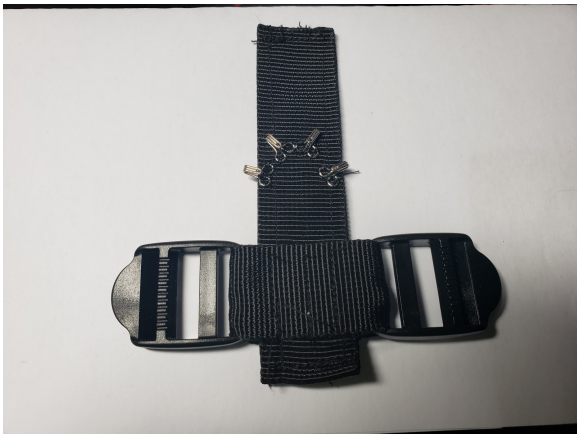


Figure 19 (Left): The two connected Ladder adjusters with the 4.5” strip, viewed from the back
Figure 20 (Right): The two Connected Ladder Adjusters with the 4.5” Strip, viewed from the top

The three inch straps must be folded in half over the remaining 12” and 8” straps to fasten them to ladder adjusters. This forms the front-arm assemblies (Figure 21). Note that the left and right front-arm assemblies are mirror images of each other.

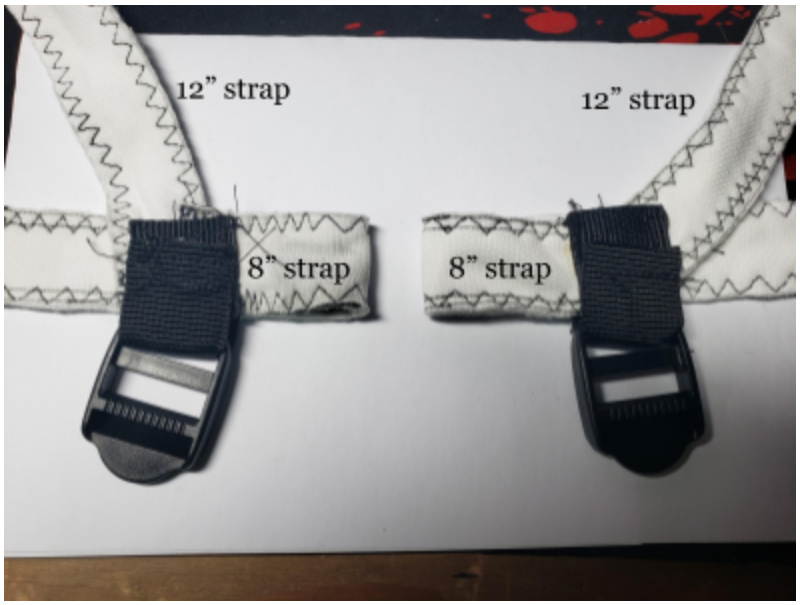

Figure 21: The front-arm assemblies, with straps labeled.

The 1” strips are just used to provide support for the strap junctions on the back. Straps should be sewn together in the following orientation with the 1” nylon strips on top. This forms the back-arm assemblies (Figure 22). Note that the left and right back-arm assemblies are mirror images of each other.

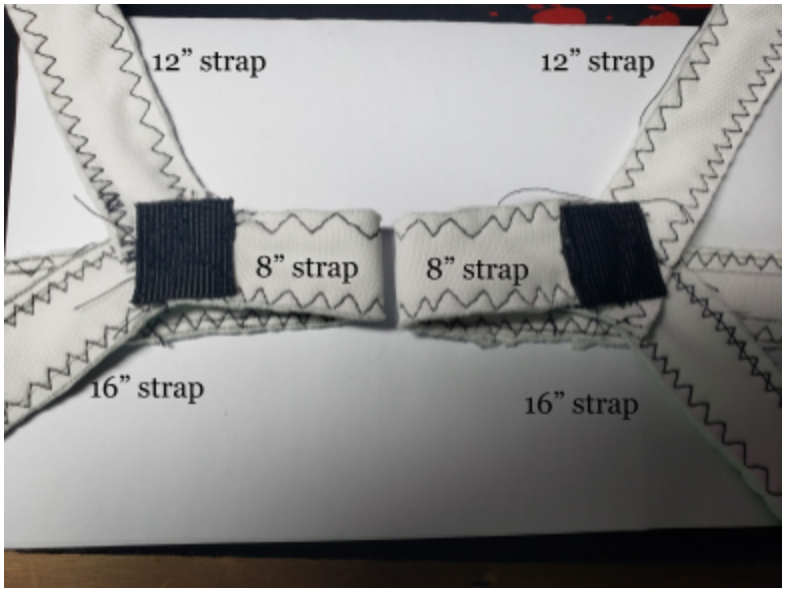

Figure 22: The back-arm assemblies, with straps labeled.

With all sewing done, final assembly can be completed. The front-arm assemblies should have their 8” straps threaded through the buckle assembly’s adjusters (Figure 23).

Figure 23: The assembly of the buckle and front-arm assemblies.

The 16” straps from the front-arm assemblies should next be threaded through adjusters on the shoulder assemblies (Figure 24).

Figure 24: The addition of the shoulder assemblies.

The 8” straps from the back-arm assemblies should be threaded through the connectors on the spine assembly (Figure 25).

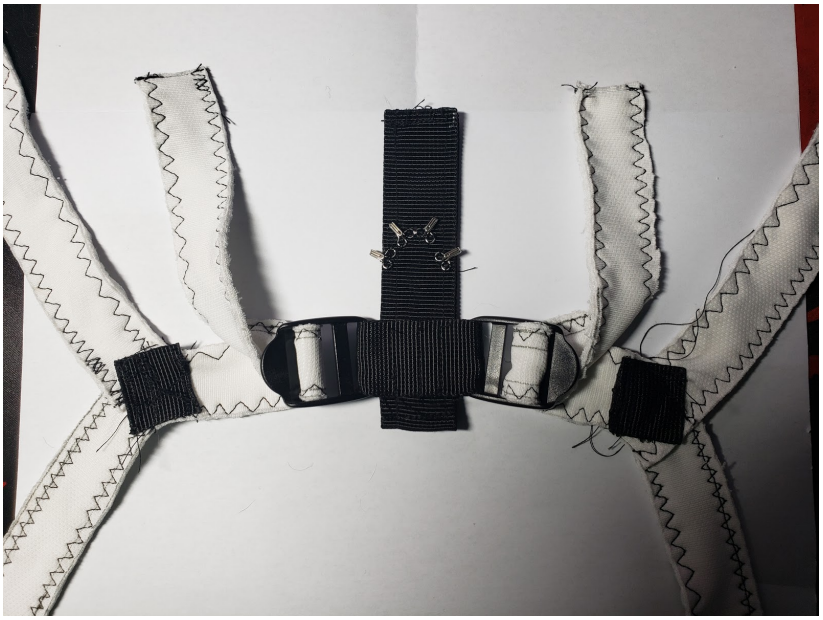

Figure 25: The assembly of the spine and back-arm assemblies.

The 12” straps from the back-arm assemblies should be threaded through the last empty adjusters on the shoulder assemblies (Figure 26), and the 16” straps from the back-arm

assemblies should be threaded through the last empty adjusters on the front-arm assemblies (Figure 27).

Figure 26: The fully-integrated shoulder assemblies.

Figures 27: The fully-integrated front-arm assemblies.

When put on a participant, each strap should lie flat, with the shoulder assemblies resting on top of the shoulders, the 16” straps resting under the arm, and the 4.5” strip in the back assembly should rest up the spine (Figure 28).

Figures 28: The fully-assembled harness on a human's back.

The final step is to connect the hooks onto the shoulder and spine assemblies so the sensors can be connected to the harness. To ensure the locations of the hooks correspond exactly to the desired fixed points (see Section 2: The Device, Harness Design - Muscle Measurements and Sensor Placement), the harness must be put on a willing volunteer. Mark the spine assembly over vertebra CVII and TI, and, after removing the harness from the volunteer, sew two sets of two hooks at 45° angle from the vertical (Figure 29). The sets of hooks on the shoulder assemblies should be centred around the centre of the nylon strips, and should also make 45° angles so they point towards the spine assembly (Figure 30). The hooks in each set should be spaced 0.5" apart.

Figure 29: The spine and shoulder assemblies with hooks attached

Figure 30: The harness on a human's back with the sensors mounted.

Appendix E: Proposed Experiment for Device Validation

Because of the fundamental importance of the topic, the induction of stress in psychological experiments is a common manipulation, with well-developed methods documented by extensive literature. There are a multitude of viable options to choose from when selecting the best test for this experiment, with each targeting different kinds of stress. This can include items such as calculation tasks, memory tasks, and logic puzzles- most commonly in the form of serial mental subtraction (Wijsman, et. al., 2013; Schleifer, et. al., 2008; Allen. Et. al, 2013). Other tests may involve an activity where participants are required to assess conflicting stimuli, such as the Stroop Color-Word Association test (Larsson et. al., 1995; Lundberg et. al., 1994). Some researchers believe a physical stimulus is more effective in inducing stress in participants. This is often done by administering a small electric shock (Krantz, et. al., 2004), or exposing the participant to something painfully cold (e.g., the cold pressor test; Mitchell, 2013). Ideally, the induction of stress also involves one or more psycho-social elements. The Trier Social Stress Test employs a public speaking event where participants must market themselves as if applying for a job (Allen. Et. al, 2013). This test has been validated by a number of studies, and is described as “the most widely used laboratory stress protocol in psychoneuroendocrinology”(Henze, et. al., 2017).

To design a well-balanced study on effectiveness of a given stress measurement technique, it is appropriate to ensure multiple types of stress are manipulated. We would recommend validating this device by using both the Trier Stress Test, which includes a psychosocial and cognitive challenge, and a Stroop Color-Word Test. While the Trier Test has significant documentation in the broader field of psychology, few studies have tested it in conjunction with EMG research. In contrast, while the Stroop Color-Word Test is less commonly

used as a stress manipulation, the majority of studies examining the induction of stress measured by EMG of the Trapezius use this technique. For this reason, we will use both tests to ensure valid testing conditions.

Participants:

We would recommend testing at least thirty participants, ideally across a range of shoulder widths. Participants are aware they will have sensors applied to them, and that they will be participating in a series of stress tests, but we recommend that the exact nature of the stress tests not be disclosed so as to preserve their effectiveness.

Overall Experimental Design:

This experiment is designed to manipulate participant stress levels using both the Trier and Stroop Color-Word Tests. Participants will be randomly assigned to either begin with the Stroop Color-Word Test or the Trier Test, but will complete both by the end of the study. Participant stress responses will be measured by EMG sensors, with intent to compare to the readings of the "S3" (Soft Strain Sensor) designed in-house. Each Participant's EMG scores will be normalized against their baseline EMG results, so that the true measurement being taken is change in muscle tone, not absolute muscle tone. The EMG functions to verify that the subject experienced stress, and to determine if the sensor we developed also reflects that experience. We elected not to include a self-report, as we believe the two comparative measurements should be sufficient, and because we are replicating as closely as possible two tests which are incredibly well-documented in being successful at inducing stress. Additionally, we believed asking participants after each section how stressed they were would not yield valid data and would detract from the effects we hope to produce.

Trier Stress Test. In the Trier Test, participants are informed they will have a few minutes to prepare a speech to present to a panel of interviewers (confederates helping conduct the study), with the intent of convincing them of their candidacy for their dream job. Sensor readings will be taken as participants prepare their speech, and as they perform their speech for a pair of confederates. The confederates are designed to react minimally, giving no signs of approval. This social stress task is followed by a mental arithmetic task (serial subtraction). The test is designed to activate a number of types of stress, which are historically measured through biological and psychological effects (galvanic skin response, salivary cortisol, heart rate, self-reports, cognitive performance; Allen, et al, 2013).

Stroop Color-Word Association Test. The Stroop Color-Word Association Test consists of a series of color-words presented in contrasting colored ink (the word "blue" written in red ink, or "yellow" written in black). This test is a cognitive task designed to create a disconnect between different presented stimuli as participants are asked to report only the colored ink of a word, rather than the word itself. Participants will be told they will be scored on how quickly they complete the task and how many items they say correctly. In reality, no scoring will take place. Rather, we will look at the stress measurement collected by EMG and the S3 sensor.